

SPATIOTEMPORAL RESPONSE DYNAMICS OF CORTICAL NEURON  
POPULATIONS IN RAT SOMATOSENSORY CORTEX

Andrew P. Brna

A dissertation submitted to the faculty at the University of North Carolina at Chapel Hill in  
partial fulfillment of the requirements for the degree of Doctor of Philosophy in the  
Department of Biomedical Engineering (Neuroscience).

Chapel Hill  
2017

Approved by:

Oleg Favorov

Jeffrey Macdonald

Lianne Cartee

Robert Dennis

Mark Tommerdahl

© 2017  
Andrew P. Brna  
ALL RIGHTS RESERVED

## **ABSTRACT**

Andrew P. Brna: Spatiotemporal Response Dynamics of  
Cortical Neuron Populations in Rat Somatosensory Cortex  
(Under the direction of Oleg Favorov)

Sensory testing offers sensitive means of assessing brain health. In particular, spatiotemporal patterns of vibrotactile stimulation of fingertips have been shown to be highly effective in probing cerebral cortical machinery involved in perception and detecting its abnormalities in a variety of neurological disorders.

In this study, extracellular spike discharge activity was recorded in microelectrode penetrations of primary somatosensory cortex (SI) in 12 rats while stimulating tips of contralateral index and middle fingers. These data were collected at 42 recording sites in the two macrocolumns responsible for processing tactile information from the stimulated fingertips. Two computer-controlled vibrotactile stimulators delivered 15 different patterns of sinusoidal skin vibrations of amplitudes and time courses previously found effective in human sensory studies in detecting various neurological disorders. Simultaneous responses of the two macrocolumns to the same stimulus were reconstructed from the responses recorded in one macrocolumn to finger-reversed stimuli. These recordings show that a single-digit stimulus initially evokes a response in multiple macrocolumns and its amplitude is best reflected in their net mean firing rate. Next, two-digit stimulation differentially affects their macrocolumns based on relative amplitudes of the stimuli applied, with the more weakly stimulated macrocolumn being suppressed by contrast-enhancing lateral inhibition. Application of a high-amplitude conditioning stimulus to a single digit prior to two-digit stimulation greatly reduces activity at the macrocolumn corresponding to that digit

through adaptation, decreasing the relative difference between the adjacent macrocolumns despite contrast-enhancing inhibition. Meanwhile, application of a low-amplitude conditioning stimulus to both digits prior to two-digit test stimulation increases the relative difference in the responses of the two macrocolumns. Finally, a slowly ramping stimulus from subthreshold to suprathreshold amplitudes evokes slow feed-forward inhibition and decreases the overall activity of the responding macrocolumn. All these cortical behaviors well parallel perceptual effects of the same stimulus permutations reported by human subjects.

In conclusion, this study identifies and quantitatively characterizes a number of dynamic features of the neurotypical SI cortical response to standardized vibrotactile stimulation, which are expected to show significant variability in different neurological disorders, thus guiding the study of their underlying mechanisms.

## TABLE OF CONTENTS

LIST OF FIGURES .....	vii
LIST OF ABBREVIATIONS .....	ix
INTRODUCTION .....	1
CHAPTER 1: EXPERIMENTAL DESIGN AND METHODS .....	6
Section 1.1 - Cortical Responses and Dynamics Under Study .....	7
Section 1.2 - The Rat Model and the Forepaw Barrel Subfield .....	10
Section 1.3 - Subject Preparation .....	11
Section 1.4 - Extracellular Recordings and Stimulus Protocols .....	13
CHAPTER 2: CORTICAL REPRESENTATION OF STIMULUS AMPLITUDE .....	20
Section 2.1 - Response to Stimulation .....	21
Section 2.2 - Representation of Amplitude .....	24
Section 2.3 - Response in Adjacent Cortical Region .....	26
Section 2.4 - Implications for Perception of Amplitude .....	29
CHAPTER 3: RESPONSES TO SIMULTANEOUS TWO-DIGIT STIMULATION .....	38
Section 3.1 - Single vs. Two-Digit Stimulation .....	39
Section 3.2 - Effects of Single-Site Conditioning .....	45
Section 3.3 - Effects of Dual-Site Conditioning .....	47
Section 3.4 - Impact of Conditioning on Amplitude Discrimination .....	51
CHAPTER 4: REDUCTION OF CORTICAL ACTIVITY THROUGH DYNAMIC STIMULATION .....	59
Section 4.1 - Neurological Basis for Feed-Forward Inhibition .....	60

Section 4.2 - Cortical Response to Ramping Stimulation .....	61
Section 4.3 - Impact of Feed-Forward Inhibition on Perception.....	65
CONCLUSIONS.....	69
REFERENCES.....	71

## LIST OF FIGURES

Figure 1.1: Examined Response Dynamics .....	7
Figure 1.2: Digit Platform and Stimulus Probe Setup .....	14
Figure 1.3: Stimulus Protocols .....	16
Figure 2.1: Average Neuron Response to Stimulation of Different Amplitudes .....	22
Figure 2.2: Average Neuron Response per Stimulus Cycle.....	23
Figure 2.3: Average Neuron Response to Stimulation at Adjacent Digit .....	27
Figure 2.4: Distribution of Responses with Low-Amplitude Stimulation .....	31
Figure 2.5: Combined Macrocolumn Responses at Suprathreshold Amplitudes.....	34
Figure 2.6: Representation of Stimulus Amplitude at Cortical Level.....	36
Figure 3.1: Macrocolumn Responses to Stimulation at 1 or 2 Digits .....	40
Figure 3.2: Marginal Macrocolumn Response to Principal Digit and Two-Digit Stimulation .....	42
Figure 3.3: Digit Macrocolumn Responses to Two-Digit Stimulation.....	43
Figure 3.4: Principal Macrocolumn Response Following Single-Site Conditioning .....	45
Figure 3.5: Principal Macrocolumn Response Following Dual-Site Conditioning.....	47
Figure 3.6: Digit Macrocolumn Responses Following Dual-Site Adaptation .....	50
Figure 3.7: Time Courses as Source of Amplitude Discrimination Performance.....	51
Figure 3.8: Macrocolumn Comparisons for Amplitude Discrimination.....	53
Figure 4.1: Average Neuron Response with Ramping Stimulation .....	62
Figure 4.2: Distribution of Responses with Ramping Stimulation.....	64

Figure 4.3: Cortical Response to Static vs. Ramping Stimuli ..... 66

## LIST OF ABBREVIATIONS

AD	amplitude discrimination
DSc	dual-site conditioning
FBS	forepaw barrel subfield
FFI	feed-forward inhibition
KS	Kolmogorov–Smirnov
MFR	mean firing rate
NGF	neurogliaform
OIS	optical intrinsic signal
OMFR	overall mean firing rate
QST	quantitative sensory testing
RF	receptive field
SI	primary somatosensory cortex
SSc	single-site conditioning

## INTRODUCTION

Early analyses of patient pain were qualitative in nature, commonly involving patient self-reporting of symptoms. Such tests were poorly defined, not directly comparable among patients, and arguably unreliable; this made them difficult to use in medicine and unhelpful in research. The need to create standards for comparison and to improve repeatability in the field of pain lead to the development of quantitative sensory testing (QST) for better diagnosis and monitoring (for review, see Roldan and Abdi, 2015). QST is a research technique involving the application of known stimuli at the periphery and the recording of one or more resulting metrics. The metrics produced by QST have measured numerical values, rather than self-reported descriptions, and they are reflective of aspects of nervous system function and health.

Through QST, pain became quantifiable, and diagnosis and monitoring could be done by comparing recorded metrics to known, standard values. However, the types of stimuli utilized in early QST tests could only probe the peripheral nervous system and spinal cord, and QST metrics were limited to quantifying pain. In recent years the use of QST has spread beyond pain and into touch, and new testing protocols have allowed for the quantification of cortical function as well (Tommerdahl et al., 2010; Verberne et al., 2013).

Newer QST protocols commonly involve the use of vibrotactile stimulation, which is the application of sinusoidal vertical displacement waveforms of specified parameters via one or more tactile probes to the surface of the skin (Puts et al., 2013). Following the application of each waveform, subjects are asked to make a choice or react to the stimulus in some way, and through repetition and systematic waveform alteration, the tests converge asymptotically to the value of the

metric under observation (e.g. Tannan et al., 2007; Zhang et al., 2011b; Puts et al., 2013; Nguyen et al., 2013a).

Different metrics can be recorded using QST testing by varying the testing pattern or adding a confounding element to the stimuli. Three metrics commonly collected are reaction time, amplitude discrimination, and dynamic threshold; each is captured using a different testing paradigm. Reaction time is the simplest of these, measuring the amount of time between the application of a stimulus to one fingertip, or digit, and the subject's perception thereof as indicated by a voluntary action, such as clicking a button (Zhang et al., 2011b). Amplitude discrimination uses a more complex protocol, applying two stimuli of different amplitudes to two different digits and asking the subject to choose which stimulus felt stronger (Tannan et al., 2007). The metric recorded is the minimal amplitude difference between the stimuli at which the subject can accurately complete the test. Altering the duration of one or both stimuli will change the metric's value in a healthy subject. Lastly, dynamic threshold is itself a variant of static threshold (Zhang et al., 2011b). The static threshold metric is the weakest stimulus a subject can reliably detect as determined over the course of multiple tests, each using a unique stimulus of unchanging amplitude. In comparison, dynamic threshold instead slowly ramps up a single stimulus, and the amplitude at which the subject detects the stimulus is recorded as the metric.

Studies conducted at many different research institutions have shown that QST metrics in those with atypical or altered brain function deviate from typical values. A wide assortment of neurological populations have been examined using QST over the past decade and a half, and in each case, the population could be statistically differentiated from neurotypical controls through examination of one or more QST metrics. Autism spectrum disorder (Tannan et al., 2008, Tavassoli et al., 2016), migraines (Nguyen et al., 2013c), chronic alcohol use (Nguyen et al., 2013b), chronic pain (Zhang et al., 2011a), pharmaceutical use (Folger et al., 2008), Parkinson's disease (Kursun et

al., 2013), type 2 diabetes (Favorov et al., 2017), and mild traumatic brain injury (mTBI)/concussion (Tommerdahl et al., 2016) are just a few of the cortical developments, injuries, and disorders that have been studied using QST techniques, and the list is ever-expanding. QST metrics of certain populations have even been shown to change over the course of treatment; in mTBI studies, the return of affected QST metrics to baseline correlated well with patient recovery (Ketcham et al., 2014). These results support the use of QST metrics as both diagnostic and monitoring tools for cortical dysfunction.

QST metrics are able to identify and monitor cortical dysfunction because they are reflective of the operation and dynamics of the cortex's underlying machinery (Tommerdahl et al., 2010). The function of the cortex is reliant on numerous mechanisms that operate within local neuronal populations, and those mechanisms are shared across the cerebral neocortex. If the base mechanism of a cortical dynamic effect is changed, the effect would be compounded through repetition, resulting in a system-level disorder. Therefore, QST metrics are able to identify atypical developments, injuries, and disorders because those conditions disrupt the mechanisms of local neuron populations that QST metrics are specifically designed to examine (Tommerdahl et al., 2010). By examining QST results, it is possible to non-invasively probe the nervous system and discern which cortical mechanisms are affected and to what degree.

Different QST metrics are designed to take advantage of specific behaviors of cortical neurons populations *in situ*. For example, reaction time is the result of a three-step process, reflecting the time required for a tactile signal to be transmitted to the cortex, the signal to be perceived, and a motor signal to be transmitted to the muscles. In addition to reflecting nerve conduction speed, reaction time tests check that the nervous system is functioning as a whole with proper communication among its parts. A disruption in communications would affect the recorded metric (e.g. Zhang et al., 2011b).

In comparison, amplitude discrimination examines adaptation, lateral inhibition, and the funneling phenomenon among cortical neurons (Simons et al., 2007). Funneling is a spatiotemporal phenomenon wherein the initial, broad response seen in a population of neurons narrows with extended stimulation, likely due to the effects of activity-driven lateral inhibition on the edges of the response (Tommerdahl et al., 2010). When a vibrotactile stimulus is first applied, the majority of neurons within linked to the stimulated region become activated, but as time passes, only those neurons most strongly activated by the stimulus continue firing, though through adaptation their activity progressively falls (Whitsel et al., 2003). Meanwhile, the activity of surrounding neurons drops even further due to lateral connections among them, increasing spatial contrast (Simons et al., 2007). Increasing the duration of the stimuli allows more inhibition to occur, which functionally isolates the two applied stimuli and improves discriminative ability (Tannan et al., 2007). If lateral inhibition or adaptation do not function as expected, the QST metric will deviate from expected values (e.g. Tannan et al., 2008; Tommerdahl et al., 2016).

Dynamic threshold tests examine the feed-forward inhibition (FFI) mechanism, which affects a subject's ability to perceive a given stimulus (Zhang et al., 2011b). FFI is a temporal phenomenon wherein the same drive from the periphery that causes excitation in cortical neurons will also promote their suppression through more sensitive inhibitory neurons (Miller et al., 2001). Compared to a static threshold test where a supra-threshold stimulus causes immediate firing of neurons in somatosensory regions at levels promoting perception, the slow ramping stimulus in a dynamic threshold test likely diminishes initial neuron firing (Zhang et al., 2011b). With the ramping stimulus, a higher amplitude of stimulation is required to produce the same firing rate. The dynamic threshold metric is able to recognize changes in this effect (e.g. Favorov et al., 2017).

The purpose of this work was to quantify the spatiotemporal response dynamics of cortical neuron populations underlying QST metrics such as these. Using electrode recordings techniques

the effects of amplitude discrimination and dynamic threshold stimuli on local neuron populations will be characterized in healthy rat populations. This work will better define the basis for QST metrics and provide valuable insights into the cortical mechanisms that drive them.

Sprague Dawley rats were used as the primary animal model for these studies. The primary somatosensory cortex (SI) in rats is organized as a set of well-defined units referred to as barrels. As described above, the testing protocols to be used here involve the stimulation of one or more digits, and in rats there exists a single barrel, or macrocolumn, that processes afferent inputs from a given digit tip (Waters et al., 1995). Having one region of cortex that services a single digit, as opposed to multiple regions, allowed for easier interpretation of the effects of digit stimulation and aided in region identification during testing. This allowed for simpler data collection, more meaningful processing, and improved reproduction of results across multiple subjects.

The research detailed in this work examines the spatiotemporal response dynamics of cortical neurons with the intent of understanding the operation of the mechanics that drive them. These mechanics ultimately power our ability to perceive our environment, and by quantifying their typical effects on cortical activity, we can better identify and characterize atypical operations. The results and analyses presented here will lead to more informative diagnoses and better management of cortical developments, injuries, and disorders.

## CHAPTER 1: EXPERIMENTAL DESIGN AND METHODS

Numerous human perceptual studies have shown that the perceptions of certain stimuli can have different properties from those actually applied (e.g., Tannan et al., 2007; Zhang et al., 2011b), suggesting that the cortex transforms the raw information from skin mechanoreceptors before conscious perception actually occurs. Extracellular recordings and optical intrinsic imaging studies using simple, single-digit stimulus patterns confirmed that activity in SI does not perfectly reflect applied stimuli, and it instead generates dynamics with spatial and temporal components that alter stimulus cortical representations (Whitsel et al., 2003; Simons et al., 2007; for review, see Tommerdahl et al., 2010).

Interestingly, applied stimuli with characteristics specifically designed to exploit such dynamics have been shown to produce altered percepts in populations with underlying cortical dysfunction, including but not limited to those with neurodevelopmental disorders (Tannan et al., 2008, Tavassoli et al., 2016), hypersensitivity and chronic pain (Zhang et al., 2011a; Nguyen et al., 2013c), pharmacological manipulation (Folger et al., 2008; Nguyen et al., 2013b), and cortical injury (Tommerdahl et al., 2016). However, while earlier studies did confirm the existence of certain cortical dynamics, the stimuli used were simple; to date, no research has directly examined the cortical effects of such stimulus patterns sensitive to changes in the cortical mechanisms that result in atypical function.

Towards that end, the purpose of this study was to directly examine the spatiotemporal response dynamics in the primary somatosensory cortex (SI) in neurotypical subjects. Through the use of extracellular recordings made in regions of the rat SI corresponding to adjacent forelimb

digits, this study quantified changes in cortical activity evoked by standardized vibrotactile stimulation in a healthy population. The information collected and analyzed in this study forms baseline dataset against which similar data collected in disordered populations can be compared, thus guiding the study into the cortical mechanisms disrupted within such populations.

This first chapter discusses the specific spatiotemporal dynamics examined in subsequent chapters. Additionally, the steps followed to collect the data analyzed are explained to allow for subsequent repetition, and systematic alteration, of the testing procedure in future studies such as those previously suggested.

### Section 1.1 - Cortical Responses and Dynamics Under Study

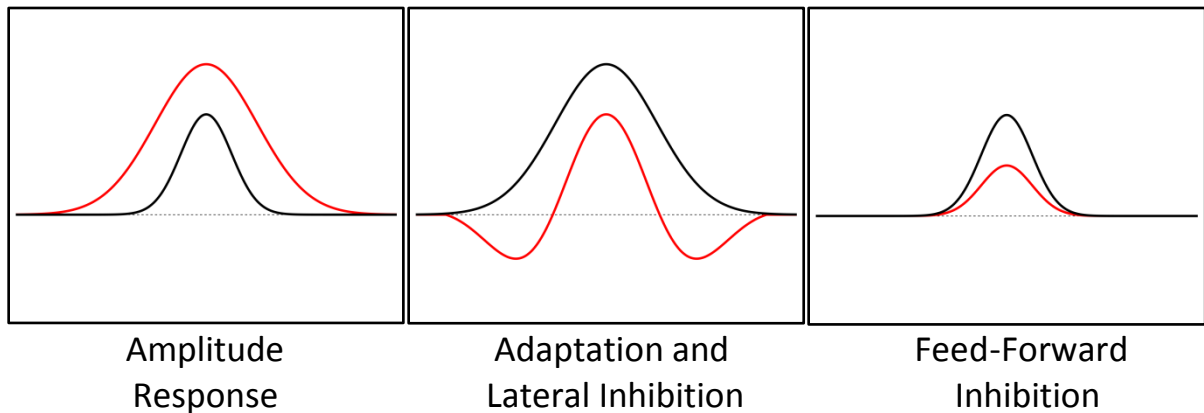


**Figure 1.1: Examined Response Dynamics**

In this study, three cortical responses with spatial and temporal components were studied. The first, illustrated in the left panel of Fig. 1.1, was that of amplitude response; the black line represents the expected cortical response to a low-amplitude stimulus, while the red line represents the expected response to a higher-amplitude stimulus. In Fig. 1.1, the vertical dimension is relative cortical activity, and the horizontal dimension is a relative spatial dimension, wherein the center of the figure is the cortical region innervated by the stimulated site, and the edges of the figure are neighboring cortical regions less innervated by the stimulated site (if at all); the dotted black line

represents the relative zero point, or background activity. Each region of the skin projects to one or more characteristic cortical modules or functional units in SI in accordance with somatotopy (Favorov and Diamond, 1990), and indirect optical intrinsic signal imaging studies have suggested that stimuli of increasing amplitudes will activate those only modules, with the overall levels of activity in those modules increasing accordingly (Simons et al., 2005). However, optical studies examining the time courses of cortical stimulus-evoked activity suggested that during early times of stimulation, a larger portion of the cortex than that representing the stimulated region becomes active, and with increased stimulus duration the activated region condenses, or "funnels" down to the final, originally-predicted region (Simons et al., 2007). Chapter 2 examines the effects of stimulus amplitude on the cortical response in adjacent cortical regions, including both the region corresponding directly with a single stimulated digit as well as that of an adjacent, non-stimulated digit, and the results therein support the existence of the initial spread of a funneling response.

The second spatiotemporal dynamic examined in this study was that of the cortex responding to stimuli of extended duration. Such a response has two dynamical features: adaptation and lateral inhibition. The middle panel of Fig. 1.1 illustrates such two-component dynamic, with the black line representing the response to a single stimulus of some amplitude for a shorter duration and the red line representing the response to a single stimulus of an extended duration. Adaptation is the progressive reduction in activity of firing neurons, akin to fatigue (Whitsel et al., 2003); in the panel in Fig. 1.1, it can be seen as a reduction in the central, most-innervated cortical regions, though it would affect all regions with activity. Meanwhile, lateral inhibition, which was first proposed following observations in sensory experiments (von Békésy, 1965) and may be related to the funneling behavior described above (Simons et al., 2007), can be seen in the two dips below background levels. Lateral inhibition results from high levels of activity at a single cortical region, which then suppresses activity below background levels in functionally-

adjacent regions with extended stimulation. Lateral inhibition is believed to be a contrast-enhancing mechanism, increasing the difference in cortical representation to stimuli applied at more than one location. Chapter 3 examines the effects of simultaneous stimulation at two functionally-related skin sites, and it compares the results of such tests to those with different types of conditioning stimuli. The stimulation of two skin sites simultaneously probes the lateral inhibition or funneling dynamics, while the conditioning stimuli apply adaptation on top of additional funneling. The results of that chapter support the theory that different conditioning stimuli can alter the contrast between different cortical regions, thus likely changing the relative perceptions of subsequent, simultaneously-applied stimuli.

Lastly, this study uses a stimulus that ramps from subthreshold to suprathreshold levels to examine the effects of feed-forward inhibition (FFI) on the cortex. Shown in red in the right panel of Fig. 1.1, FFI was expected, and eventually shown in Chapter 4, to reduce the cortical response at a given stimulus amplitude as compared to a stimulus delivered at a single, constant amplitude, shown in black. Inhibitory cells in the cortex are known to become active with weaker afferent drive than excitatory cells (Kyriazi and Simons, 1993; Kimura et al., 2010; for review, see Miller et al., 2001), thus becoming more active at lower stimulus amplitudes, but for some cell types, such as the neurogliaform (NGF) cell, inhibition can require hundreds of milliseconds to become effective (Tamás et al., 2003; Oláh et al., 2009; for review, see Overstreet-Wadiche and McBain, 2015). Perceptual studies have shown that a ramping stimulus, designed to evoke FFI by giving adequate time for inhibition to develop, will increase the detection threshold of healthy subjects (Zhang et al., 2011b), but this study is the first to examine the cortical effects of such a stimulus directly.

## **Section 1.2 - The Rat Model and the Forepaw Barrel Subfield**

The rat somatosensory cortex is uniquely suited for the systematic study of spatiotemporal response dynamics by virtue of its organization. It is generally believed that the somatosensory cortex is arranged as a mosaic of repeating units (Favorov and Whitsel, 1988; Favorov and Diamond, 1990). These units, referred to as macrocolumns or segregates, comprise 300-400  $\mu\text{m}$ -diameter clusters of vertically-oriented strands of cells with similar receptive field (RF) and sensory modality properties (Favorov and Diamond, 1990). It has been theorized that macrocolumns form the basic processing unit of the cortex (Mountcastle, 1978); as macrocolumns have been shown in modeling studies to be capable of complicated, non-linear transformations and learning (Favorov and Kursun, 2011), it is likely that macrocolumns in the somatosensory cortex perform first-stage processing of afferent information.

In larger animals such as monkeys (Powel and Mountcastle, 1959; Favorov and Whitsel, 1988) and cats (Mountcastle, 1957; Favorov and Diamond, 1990), the cortical representation of a single digit of the forelimb is known to be spread over multiple macrocolumns. All the cells within a macrocolumn share a common RF location on the skin, called the minimal RF, and the minimal RFs of adjacent macrocolumns have been shown to be non-overlapping and non-contiguous. Different parts of a single digit are primarily serviced by different macrocolumns. Such an arrangement of macrocolumns is not conducive to extracellular recordings to standardized stimuli. Stimulation of a single digit would likely activate cells in different macrocolumns in a way not immediately reproducible between subjects, and the levels of activation would be unpredictable based on the exact location of the stimulus on the skin relative to any given recording site's minimal RF.

Therefore, what makes the rat model useful for studies such as this one is that the tips of each digit are thought to be processed by a single macrocolumn each. Histological studies have revealed an area of the rat somatosensory cortex wherein the cells in the input layer form distinct

clusters, or barrels (Waters et al., 1995). Within this region, called the forepaw barrel subfield, each barrel has a minimal RF corresponding to a single glabrous pad upon the contralateral forepaw; in turn each glabrous pad is largely represented by only a single barrel. Additionally, the barrels corresponding to the digit tips are physically adjacent to one another in a line. Descriptions of the properties of rat cortical barrels match those of macrocolumns in other species, so it is highly likely that they are the same cortical structure.

This study aimed to examine the spatiotemporal response dynamics of one or more adjacent macrocolumns, and for that purpose the rat model is ideal. In comparison to other mammalian studies, using a rat model would improve reproducibility, allowing the same two macrocolumns to be studied across subjects using minimal RFs as guides. Also, stimulation at a single digit would likely produce a reliable, comparatively uniform response in the innervated macrocolumn, since each macrocolumn represents an entire glabrous pad, rather than just a component. In this study, stimulation was applied to the glabrous pads of digits 2 and 3, as both digits would have macrocolumns corresponding to adjacent digits nearby (as opposed to other, less functionally comparable regions).

### **Section 1.3 - Subject Preparation**

All animal handling and surgical and experimental procedures performed here were reviewed and approved by an institutional committee prior to initiation of the research study.

In this work, microelectrode recordings were collected in 12 healthy adult Sprague-Dawley rats (3 male, 9 female). For each experiment, anesthesia was induced with 4% isoflurane; induction took place within a covered rat induction chamber. Anesthesia and airflow were controlled using a low-flow anesthesia system (Kent Scientific SomnoSuite®). Following induction, the subject was moved to a heated surgical table, and its trachea was intubated. Anesthesia was changed to 2-2.5%

in 50/50 nitrous oxide and oxygen for the duration of surgery, and the animal was allowed to breathe naturally. Heart rate, breathing rate, and body temperature were monitored and recorded (Kent Scientific PhysioSuite®). After intubation, surgical access points were coated with local anesthetic and sutured shut.

Next, the right side of the skull was exposed, and a rectangular window was sketched onto the surface of the bone. The window was marked 2mm anterior and posterior to the coronal suture and from 1mm lateral to the sagittal suture to the edge of the skull. The majority of material in the top, left, and bottom edges of the window was triturated using a rotary tool (diamond tip, 1mm diameter); an additional edge was made by triturating a line approximately 1mm down off the right side of the skull in a shelf-like fashion. This window was not removed at this stage of the surgery.

During the electrophysiological phase of the experiment, the subject was held in place using a unique recording chamber attached to the skull. The recording chamber was designed with a circular lip at the top that could be locked into the recording setup, and the inside of the chamber tapered from 20 mm at the top to 12.5 mm at the bottom where it made contact with the skull. The chamber was bonded to the skull using dental acrylic, but as the bottom diameter of the chamber was wider than the side of the skull exposed, additional semi-rigid dental acrylic was applied to the side of the skull below the right edge of the window and allowed to dry to form an additional anchor point. When fully applied, the recording chamber was centered on the (unopened) window and was watertight at the bottom.

A silver reference electrode was inserted into the facial muscle and sutured into place. Afterwards, the exposed surgical areas were coated with local anesthetic and sutured shut. The reference electrode was then moved around the ear to prevent movement artifacts during electrophysiological recordings. The subject was subsequently moved to the heated experimental

platform where the recording chamber was locked into the recording setup and aligned appropriately along an anterior-posterior axis.

Finally, the remainder of the window was removed, and in some experiments the dura was resected. Artificial cerebrospinal fluid was added to the recording chamber to keep the cortex moist, and images of the cortex were taken for anatomical reference. After this, electrophysiological data were collected as described below utilizing vibrotactile stimulation of the contralateral forepaw. Upon commencement of data collection, isoflurane levels were adjusted to minimal levels that would sustain general anesthesia (usually 0.3-0.6%). Following data collection, the subject was euthanized with 5% isoflurane and opening of the chest cavity.

#### **Section 1.4 - Extracellular Recordings and Stimulus Protocols**

Extracellular recordings were made in the forepaw barrel subfield of the right somatosensory cortex in response to stimulation of the contralateral forepaw. A tungsten microelectrode (FHC, Inc.) was inserted into the cortex at a near-radial orientation using an electrode driver, and extracellular cortical action potentials ("spikes") were monitored using external speakers connected to recording equipment and graphic display. Extracellular spikes were conditioned and amplified through first-stage multi-channel recording equipment (Alpha Omega MCP-Plus 8), and resulting analog signals were viewed and saved for post-processing through second-stage recording equipment (Alpha Omega AlphaLab Pro). The recording setup was controlled through a dedicated lab computer, and the data were sampled and saved at 25 kHz.

Spike discharge recordings were made at depths corresponding to the middle and deep cortical layers; the correspondence between depth and recording layers was confirmed through histological examination of small electrolytic lesions made at recording sites. Typically recordings were made at 2 depths per penetration, for a total of 42 recording sites in 24 penetrations over 12

test subjects. On average, 4-5 neurons could be discerned at each recording site, for an estimated total of 176 observed neurons.



**Figure 1.2: Digit Platform and Stimulus Probe Setup**

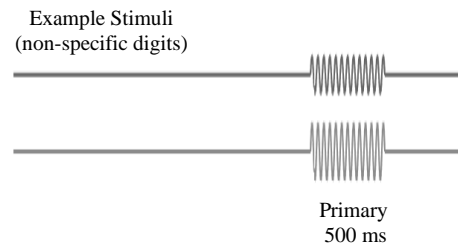
At each potential recording site, the minimal receptive field of the neurons within that site was determined through the use of punctuate stimuli delivered using von Frey filaments of progressively decreasing forces, according to procedures described in earlier work (Favorov et al., 1987; Favorov and Diamond, 1990). When a recording site was found whose minimal RFs corresponded to the glabrous pad of digits 2 or 3 as described in Section 1.2, the recording chamber was filled with agar to prevent cortical pulsations and to stabilize the recording setup further. At this time the backs of the claws or the dorsal surface of digits 2 and 3 were immobilized on separate platforms as shown in Fig. 1.2, and the platforms were weighed down with plasticine. Care was taken to ensure the digit platforms were not in contact with one another to prevent mechanical signal transmittance between the digits. By convention, the digit where the minimal RF of a given recording site was located was termed the principal digit, and the other was termed the marginal digit.

The glabrous pads at the tips of digits 2 and 3 were exposed to a total of 15 sinusoidal skin vibration patterns shown in Fig. 1.3 using separate, custom, computer-controlled vibrotactile mechanical stimulators (Cortical Metrics CM-4), and the coincident cortical activity was recorded. The frequency of all applied stimuli was 25 Hz, within the flutter range of perception (<50Hz). The stimulators were controlled using custom MATLAB (Mathworks) scripts and monitored and recorded post-experiment trial identification using additional channels of the microelectrode recording equipment. Similarly to the digit platforms, the stimulator probes were mounted on separate boom arms and were not allowed into contact during recording to prevent mechanical signal transmittance between the digits, as shown in Fig. 1.2. Probe tips were 2 mm in diameter, covering stimulated digit pads almost completely, and prior to application of stimulus patterns they were indented 500  $\mu\text{m}$  into the skin to ensure good contact.

The 15 stimulus patterns applied to the digit tips, shown in Fig. 1.3 in sequence, were modeled after stimuli used in human perceptual studies as described in earlier parts of this chapter. Any given stimulus pattern included vibrotactile stimulation of one or two digits with the potential for a conditioning or 2-stage stimuli separated by a short period. As a general rule, the primary stimulus was the portion recorded, with other stimulus instances not being processed but instead being necessary to evoke the desired spatiotemporal dynamics. Stimuli applied included simultaneous two-digit stimulation, two-digit stimulation with single and dual-site conditioning (SSc and DSc, respectively), 1-and-2-stage single-digit stimulation, and ramping stimulation. The anticipated action of each stimulus is given above in Section 1.1 and is restated in context with results in subsequent chapters. The 15 trial patterns were executed in sequence according to their order in Fig. 1.3 with an 8 sec inter-stimulus interval between trials to allow the each effects of each stimulus on the cortex to dissipate, returning the cortex to standard function (Simons et al., 2005, 2007).

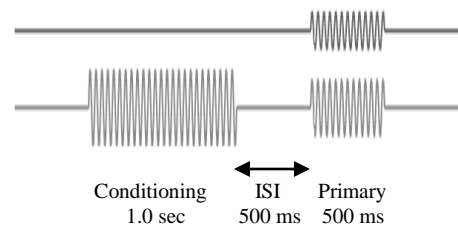
- *Simultaneous Two-Digit Stimulation* -

Principal Digit ( $\mu\text{m}$ )	Marginal Digit ( $\mu\text{m}$ )
Primary	Primary
300	200
200	300



- *Single-Site Conditioning (SSc)* -

Principal Digit ( $\mu\text{m}$ )		Marginal Digit ( $\mu\text{m}$ )	
Conditioning	Primary	Conditioning	Primary
400	300	-	200
-	200	400	300



- *Dual-Site Conditioning (DSc)* -

Principal Digit ( $\mu\text{m}$ )		Marginal Digit ( $\mu\text{m}$ )	
Conditioning	Primary	Conditioning	Primary
200	300	200	200
200	200	200	300

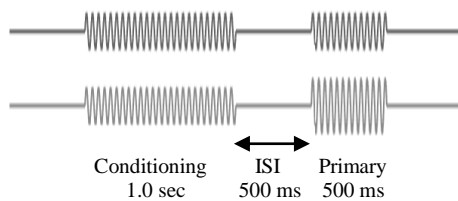
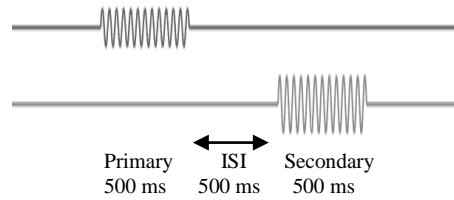


**Figure 1.3: Stimulus Protocols**  
 (All amplitudes in  $\mu\text{m}$ , peak-to-peak. All stimuli were applied at 25 Hz.)  
 (cont.->)

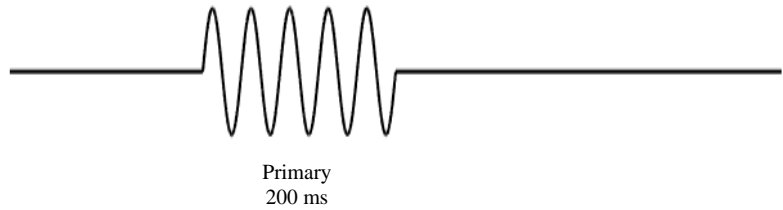
- 2-Stage Single-Digit Stimulation -

Principal Digit ( $\mu\text{m}$ )		Marginal Digit ( $\mu\text{m}$ )	
Primary	Secondary	Primary	Secondary
300	-	-	200
200	-	-	300
-	300	200	-
-	200	300	-



- 1-Stage Single-Digit Stimulation -

Principal Digit ( $\mu\text{m}$ )
Primary
12.5
25
50
75



- Ramping Stimulation -

Principal Digit ( $\mu\text{m}$ )
Primary
0 -> 80

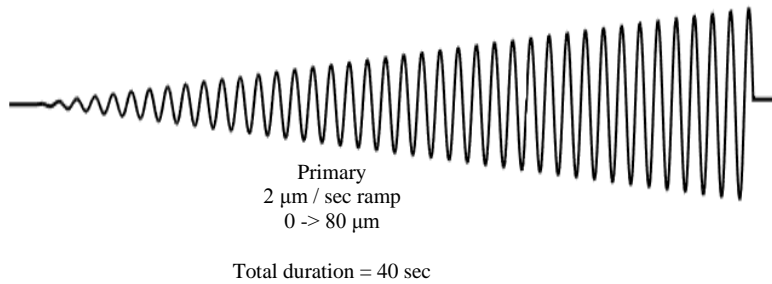


**Figure 1.3 (cont)**  
**(All amplitudes in  $\mu\text{m}$ , peak-to-peak. All stimuli were applied at 25 Hz.)**

Note that 2-stage single-digit stimulation applied stimuli to digit 2 and digit 3 in sequence, but as this study did not utilize information from during the Secondary period, the Primary stage of 2-stage single-digit stimulation should be considered equivalent to 1-stage (henceforth, both will be referred to as single-digit stimulation). Information from the secondary period of 2-stage single-digit stimulation will be used in subsequent studies regarding sequential amplitude discrimination. Additionally, the conditioning period in SSc was utilized as another example of single-digit stimulation, as the conditions of stimulation were comparable.

For a single recording site, the 15 trial patterns were applied to the digit tips 15 times, for a total of 225 trials per recording site, 15 trials per stimulus pattern. The entire battery took approximately 45 minutes, at which point a new recording site would be sought out. The data recorded during the trials were processed off-line using custom MATLAB scripts, wherein spikes were detected for 3 seconds before and after each trial. The spike detection algorithm used a slope-filter to isolate action potentials, and the timings of peaks/valleys in the recorded data with a magnitudes greater than a threshold value were recorded as spike events. To prevent the recognition of a single neuron firing twice, the larger of two spikes observed within a set period (0.57 ms) was recorded and the other discarded. Within a single recording site, the spike events were grouped in bins of varying lengths and averaged by the number of trials captured for a given stimulus pattern. These site results were then averaged with other recording sites, smoothed, and scaled by the average number of neurons per recording site. For the purposes of data analysis, recordings made in digit 2 and digit 3 recording sites were considered equivalent. Only recording sites in which a full 15 trials were obtained for a given stimulus pattern were used in data analysis.

Due to limitations in the setup used, the activity of multiple macrocolumns could not be recorded simultaneously. Instead, to reconstruct the simultaneous responses of adjacent macrocolumns for certain tests, the response at each recording site was recorded twice for a given

set of stimulus amplitudes. The first time, the amplitudes would be applied such that the larger stimulus was applied at the location of the principal digit, and the second time, the digits to which the stimuli would be applied were switched. This can be seen in Fig. 1.3 as seemingly repetition, wherein the same stimulus amplitudes and conditioning values are used in subsequent trials but the digits to which they are applied are opposite. Doing so changed the context of the recording site, with its first representing the macrocolumn directly activated by the stimulation, and its second representing the macrocolumn of a digit adjacent to that directly activated. In this manner, the simultaneous responses to stimulation at multiple, adjacent macrocolumns could be examined.

## **CHAPTER 2: CORTICAL REPRESENTATION OF STIMULUS AMPLITUDE**

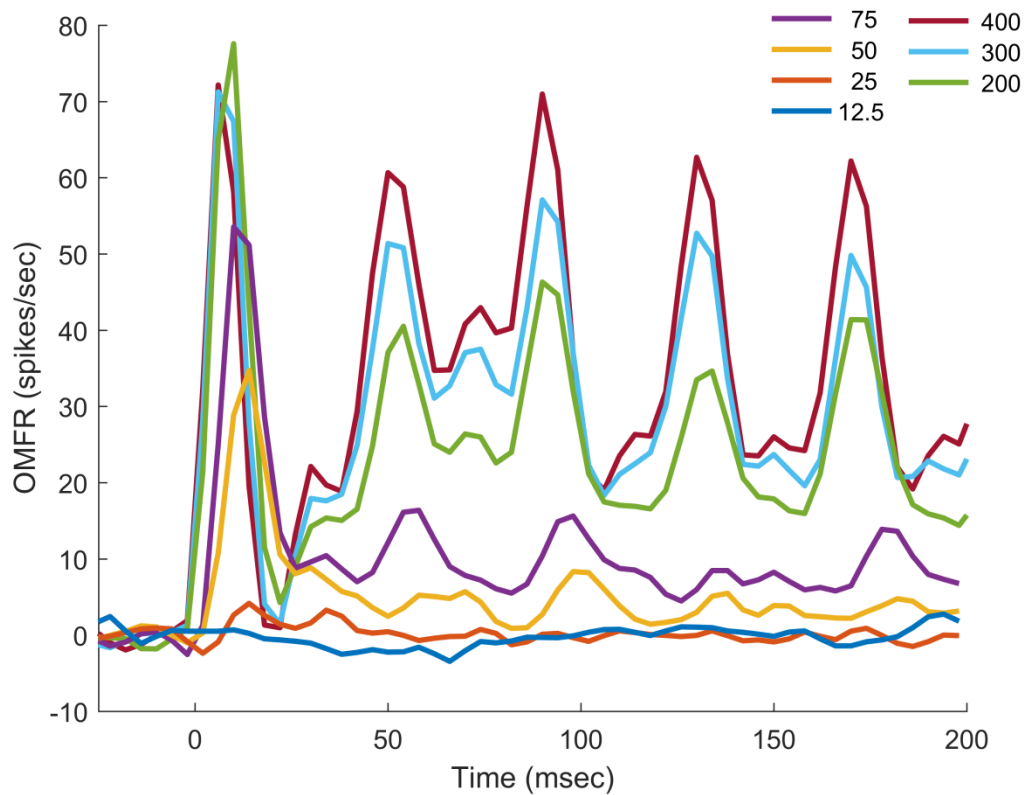
Neurons in the primary somatosensory cortex (SI), the lowest level of the cortex dedicated to processing tactile sensation, receive input from the periphery through primary afferent fibers. Displaying a firing pattern that is largely independent of stimulus amplitude, these primary afferent neurons, connected directly to mechanoreceptors in the skin, are not capable of conveying the amplitude of an applied stimulus individually (Talbot et al., 1968), though they do so through an aggregate response (Johnson, 1974; LaMotte and Mountcastle, 1975). As the amplitude of a vibrotactile stimulus can be readily perceived and determined in a continuous manner (Stevens, 1959; Talbot et al., 1968), it stands to reason that neurons at the cortical level must be able to coalesce such individual signals into a singular response from which amplitude can be discerned.

Here in Chapter 2, the population response of cortical neurons within a single macrocolumn to flutter (<50Hz) vibrotactile stimulation of varying amplitudes applied to a single digit will be examined. Unlike in earlier studies (Mountcastle et al., 1969; Whitsel et al., 2003), particular attention will be paid to the short-term time courses of cortical activity; cortical neurons are subject to temporal dynamics that alter their activity during sustained stimulation (Whitsel et al., 2003), in contrast to afferent fibers, which show little adaptation (Whitsel et al., 2000). The purpose of this study was to better detail the means by which intensity of a stimulus is coded at the cortical level, hopefully providing insights into the means by which the perception of said stimulus arises.

## Section 2.1 - Response to Stimulation

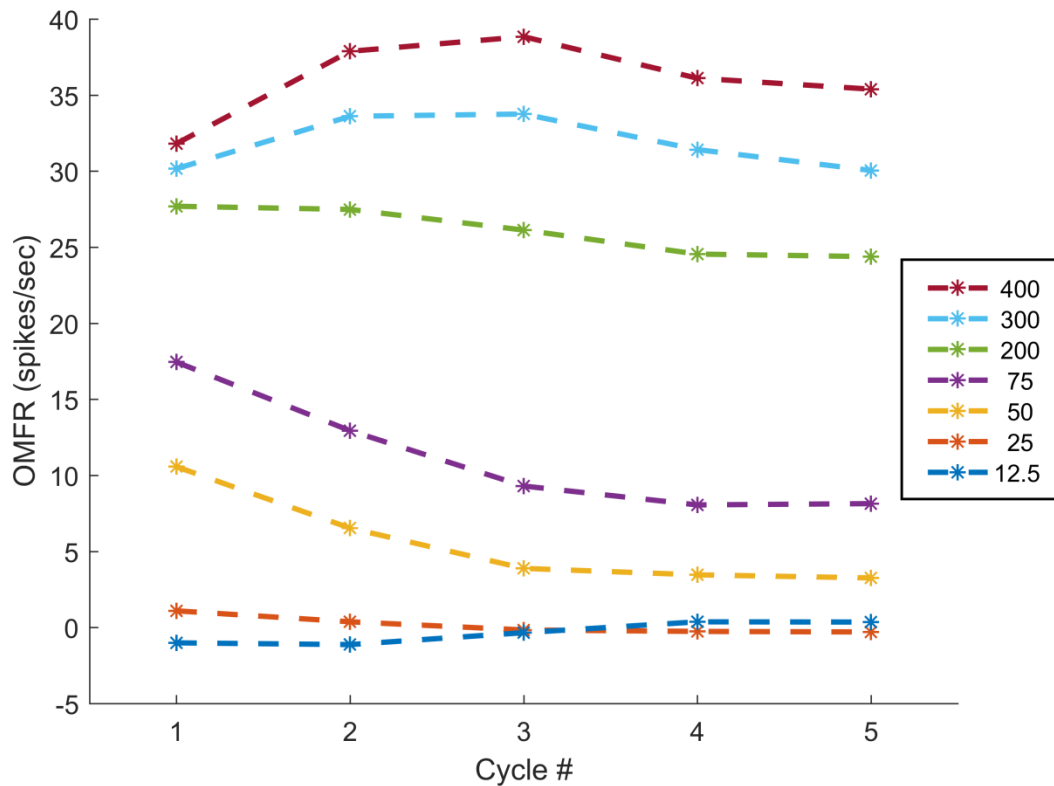
To test the effects of stimulus amplitude on SI cortical activity, a series of vibrotactile stimuli ranging from 12.5 $\mu$ m to 400 $\mu$ m were delivered to a single digit ("single-digit stimulation"). The duration of the stimuli varied from 200ms to 1000ms, but for comparison's sake only the first 200ms of stimulation will be examined here. Extracellular recordings were made at the macrocolumns whose minimal receptive fields (RFs) corresponded to either digit 2 or digit 3, with the digit where the minimal RF was located being termed the principal digit, and the other termed the marginal digit. For the purposes of this study, the macrocolumns of both digit 2 and digit 3 are considered equivalent, and the designations of principal and marginal digits are relative to a recording site's minimal RF. In later portions of the study, single-digit stimulation was applied at the marginal digit of recording sites, rather than the principal digit; in such an arrangement, recordings made would be representative of activity at the macrocolumn corresponding to that of an adjacent digit relative to stimulation.

Fig. 2.1 gives the overall mean firing rates (OMFRs) of cortical neurons recorded over the course of single-digit stimulation at the principal digit. For each stimulus amplitude, the responses of all recording sites were averaged, scaled by the average number of neurons per recording site, divided into 4ms bins, and smoothed with a moving weighted average. In each condition, the average spontaneous activity for 500ms prior to stimulation was subtracted from the waveform to better reflect the change in cortical activity; the average spontaneous firing rate for all stimulus patterns was  $13.1 \pm 0.3$  spikes/sec, which matches values seen in earlier studies (Mountcastle et al., 1969). Stimulation was applied at 25Hz at 0ms and continued for at least 200ms.



**Figure 2.1: Average Neuron Response to Stimulation of Different Amplitudes (All amplitudes in  $\mu\text{m}$ , peak-to-peak)**

It can be seen in Fig. 2.1 that all amplitudes above  $25\mu\text{m}$  follow approximately the same time-course. Prior to stimulation, cortical activity remains at a constant, spontaneous level, but activity clearly rises above spontaneous levels at all points during stimulation. Each stimulus condition shows some level of cyclical activity, the frequency of which resembles the applied 25Hz stimulus. Responses during the first cycle (40ms) of stimulation are seen as high-magnitude, sharp peaks in activity, with responses during subsequent cycles appearing as comparatively diffuse regions of lower magnitude. Additionally, as better highlighted in Fig. 2.2, the overall magnitude of each response gradually decreases with extended duration, especially after 2-3 cycles.



**Figure 2.2: Average Neuron Response per Stimulus Cycle (Stimulus cycle 40ms, all amplitudes in  $\mu\text{m}$ , peak-to-peak)**

Based on this, it can be said that the overall response patterns of SI cortical neurons to stimulation have certain components that can be expected regardless of stimulus amplitude, and these aspects begin within the first tens of milliseconds of stimulation. These include periodic elements resembling stimulus frequency, a gradual decrease in average activity, and a high initial spike in activity. The first of these components, termed entrainment, is a well-known temporal aspect of neurons in SI at higher amplitudes (for review, see Kohn and Whitsel, 2002), and it has long been believed to be the means through which stimulus frequency is expressed at the subcortical and initial cortical levels (LaMotte and Mountcastle, 1975). Entrainment of cortical neurons to the stimulus frequency will change over hundreds of milliseconds, with their overall firing pattern closely resembling the stimulus frequency, though the average moment of occurrence

during the stimulus cycle will shift (Whitsel et al., 2003). The second of the common components, best referred to as adaptation, is another temporal dynamic feature previously observed in SI cortical neurons; over the course of several seconds, adaptation can greatly reduce the response of the cortex to higher amplitude stimuli, with reductions as high as 50% having been reported. The mechanism which drives adaptation is poorly understood, but the consensus is that it is related to sustained neural activity (Tommerdahl et al., 2010). The third common component of the observed time-courses is the initial, sharp spike in activity during the first cycle. This activity spike has previously been reported in the literature (Whitsel et al., 2003, see Figs. 1-2), but its potential importance not been directly identified nor discussed to my knowledge.

## **Section 2.2 - Representation of Amplitude**

Despite the commonplace appearance of the high-magnitude spike early in stimulation, the relationship of that spike's value to the amplitude of the applied stimuli suggests it carries useful information. Firstly, the waveforms displayed in Fig. 2.1 show that the value of the early spike is greater than that of the rest of the waveform for all examined stimulus amplitudes. This effect is most likely related to adaptation, with the activity of cortical neurons within the macrocolumn being gradually reduced following activity-driven adjustment. However, by extension it can be inferred that the initial spike, hereafter termed the startle response, likely represents the mean activity of the macrocolumn before the any temporal dynamics have significantly taken effect. In this fashion, it can be thought of as the most basic response of the macrocolumn to stimulation at the periphery.

The magnitude of the startle response increases with stimulus amplitude at lower amplitudes, showing that it could be used to express stimulus amplitude at the level of the cortex. The gradual increase of the startle response with amplitude is consistent with neuron recruitment within the macrocolumn, though whether such an effect originates at the periphery or at the

cortical level is unclear (Mountcastle et al., 1969). At stimulus amplitudes of 200 $\mu$ m or above, the magnitude of the startle response remains at a fairly constant level. If the magnitude of the startle response does correlate with neuron recruitment, then this would suggest that maximal recruitment is achieved between 75 and 200 $\mu$ m. Early primate studies suggested that maximal recruitment of primary afferents occurs at approximately 100 $\mu$ m (Mountcastle et al., 1969), so there is some evidence in the literature to support this theory.

Although it appears related to stimulus amplitude, the plateau in the magnitude of the startle response with higher-intensity stimuli makes it insufficient to express the full range of behaviorally-relevant stimuli possible on its own. Based on the results of previous studies using long-duration, low-amplitude stimuli (Mountcastle et al., 1969) or using indirect means of observing cortical activity (Simons et al., 2005), the magnitude of the sustained response may be related to the cortical representation of amplitude. The waveforms shown in both Fig. 2.1 and 2.2 support this theory; in both representations, the OMFR of the observed macrocolumn increases with stimulus amplitude. This relationship is maintained for the duration of stimulation for all amplitudes above 25 $\mu$ m, including larger amplitudes wherein the startle response was equivalent. As the magnitude of the startle response is more prominent for low-amplitude stimuli, but the sustained response is more useful for high-amplitude stimuli, it is most likely that the amplitude of a stimulus is coded through the overall mean firing rate of neurons within the macrocolumn over a period of time beginning with the start of stimulation.

As an aside, it is interesting to note that for stimuli at and above 200 $\mu$ m, there is an additional spike in activity approximately 70ms from stimulus onset in Fig. 2.1 that does not match the remainder of the waveform. The spike is approximately 180° out of phase with other activity peaks, which suggests the spike is related to the frequency of the applied stimulus. Similar spikes can be seen between the more prominent peaks in subsequent cycles, but their magnitudes are

greatly reduced, and they are comparatively difficult to locate. At stimulus amplitudes above approximately 100 $\mu$ m, afferent fibers are known to fire twice within a single stimulus cycle, but as they reportedly occur in a "disorganized" manner (Talbot et al., 1968), and the activity of afferent fibers is not known to significantly change with time, they are unlikely result in such a differential effect. Instead, as it has been shown that neuron entrainment improves over the first few hundred milliseconds of stimulation at this frequency (Whitsel et al., 2003), the spike is likely indicative of a period before which the mechanisms that power cortical entrainment have taken significant effect. As with the startle response, this pre-entrainment peak suggests that the activity of cortical neurons is modulated through mechanisms that require some period of time or previous level of activity to take effect.

### **Section 2.3 - Response in Adjacent Cortical Region**

Studies with optical intrinsic signal (OIS) imaging revealed that while the spatial extent of the cortex activated following extended vibrotactile stimulation does not change with stimulus amplitude, the response of the cortex to suprathreshold stimulation does change shape with time (Simons et al., 2005, 2007). The initial response is broad, with multiple adjacent regions showing activation, while the extended response (>1sec) is narrow, with regions whose RFs best reflect the stimulated area showing activation and adjacent regions showing suppression. Such changes in the spatial response with time are cumulatively referred to as funneling (Tommerdahl et al., 2010), and they are believed to be related to long-range horizontal connections between macrocolumns and pericolumnar inhibition (Tommerdahl et al., 2010). To date, the funneling response has only been observed through indirect means such as OIS, and it has not been examined through direct techniques.

Towards that end, here the early response of a macrocolumn adjacent to that of the digit exposed to single-digit stimulation is examined directly through extracellular recordings. OIS imaging indicated that in the early stimulus response, multiple adjacent macrocolumns displayed activity; since the macrocolumns of adjacent digits in the rat cortex are themselves adjacent (see Chapter 1), it would be expected that the macrocolumn observed here would display activity during early stimulation of the adjacent digit, even in the absence of stimulation at the digit corresponding to its own RF center.

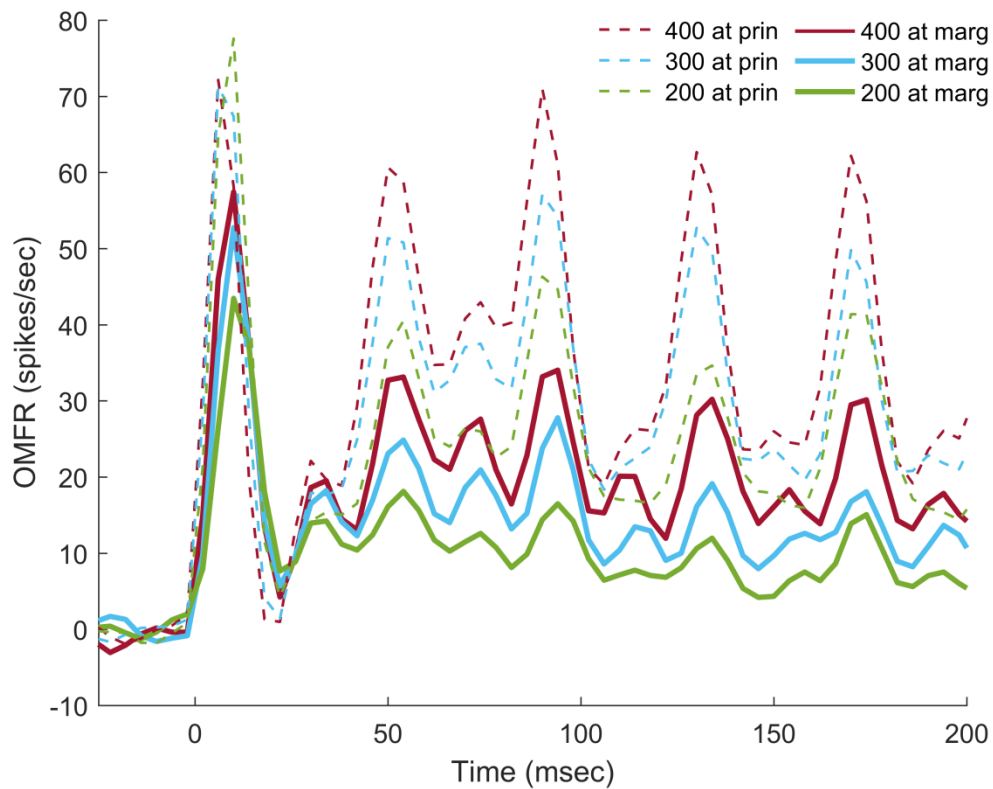


**Figure 2.3: Average Neuron Response to Stimulation at Adjacent Digit  
(All amplitudes in  $\mu\text{m}$ , peak-to-peak)**

The responses displayed in Fig. 2.3 match expectations set by previous studies regarding the funneling response. Solid lines represent the average activity of the observed macrocolumn when stimuli are applied such that it is at the marginal digit, while dotted lines, previously displayed in Fig.

2.1, show the average activity when stimulated at the principal digit. For all amplitudes tested, the activity of the macrocolumn when corresponding to the marginal digit was greater than background values for the duration of the observed testing period. This clearly illustrates that during early periods of stimulation, a greater extent of the cortex than that of the maximally stimulated region is activated. The overall magnitude of the response increased with stimulus amplitude, indicating that intense stimuli will activate adjacent areas of the cortex more strongly.

Additionally, the startle response and adaptation can be seen for each amplitude tested. This implies that as with the macrocolumn at the principal digit, the macrocolumn at the marginal digit has an initial response that is then altered through delayed temporal dynamics. The difference in magnitude of the startle response may represent a lower recruitment level in the macrocolumn of the marginal digit, which would be expected if the activity seen is caused through less direct, secondary means, such as through macrocolumn-macrocolumn connections rather than direct afferents.

Lastly, the responses of the macrocolumn of the marginal digit also display some level of entrainment to the applied stimuli. The pre-entrainment peak remains visible, but the spikes that occur between the larger peaks are more prominent than when the principal digit was stimulated, despite how their magnitudes decrease with time. This suggests that the mechanisms that lead to entrainment require more time to take effect at macrocolumns adjacent to that most strongly stimulated. Alternately, it's possible that the mechanisms that promote activity in the macrocolumn adjacent to that most strongly stimulated delay such activity, as would be expected if the adjacent macrocolumn were innervated through a longer signaling pathway. Such a mechanism could result in individual neurons in the adjacent macrocolumn initially firing at different phases early within stimulation relative to the primary macrocolumn; such a firing pattern was seen in one early test subject [data not shown].

That said, due to limitations in the original experimental design, it must be noted that conclusions regarding precise differences in magnitude or phase between representations at the principal and marginal macrocolumns during single-digit stimulation cannot be drawn at this time. During stimulation of one digit, the stimulus probe for the adjacent digit was left in contact with the skin. Though efforts were made to isolate the stimulation of a single digit (see Chapter 1), it is possible that the propagation of the stimulus wave on the skin may have caused the adjacent digit to press into the static, isolated probe in a way related to stimulus frequency and amplitude. This potential issue is unique to the rat model due to the close proximity of the digits relative to those in a primate model. However, data monitoring the movement of the stimulus probes indicate that if this effect did occur [data not shown], the amplitude of such stimulation would be well below any amplitudes that would promote cortical activity ( $\ll 12.5\mu\text{m}$ , see Fig. 2.1). The activity shown here is unlikely to have arisen from such weak stimulation. Therefore, despite this unintended limitation the conclusions drawn here regarding the funneling response remain valid.

## **Section 2.4 - Implications for Perception of Amplitude**

The amplitude of a flutter vibrotactile stimuli is perceived in a continuous manner from low to high amplitudes following a power-law relationship (Stevens, 1959). The equation governing this relationship, Steven's Power Law, states that the subjective intensity of a stimulus  $|S|$  is given by the difference between the amplitude  $A$  of a given stimulus and the detection threshold  $A_0$  of that perceptual modality, all raised to an exponent  $n$  and scaled by a constant  $\alpha$ .

$$|S| = \alpha(A - A_0)^n \quad (\text{Steven's Power Law})$$

The constant  $\alpha$  will vary based on the units used to measure stimulus intensity, but the exponent  $n$  is specific to the stimulus modality being tested. Original tests regarding the perception of

vibrotactile stimuli in humans found that the relationship was near-linear, with the exponent  $n$  having values near 0.95 for frequencies in the flutter range (Stevens, 1959; Talbot et al., 1968). Primates have been confirmed to perceive such stimuli similarly to humans (LaMotte and Mountcastle, 1975), which suggests that this relationship holds for a variety of mammals.

While this law governing perception of stimulus intensity was first proposed over fifty years ago, the means through which such a relationship is reflected at the cortical level has not yet been determined. In this final section of Chapter 2, a model utilizing spatial and temporal dynamics of SI will be proposed utilizing the overall mean firing rates of multiple macrocolumns.

Examination of the rat model has shown that the mechanoreceptors in the glabrous skin of the rat have similar properties to those of primates, and the median mechanical threshold of rat RA afferent fibers is approximately 5.60mN (Leem et al., 1993a, 1993b). Early studies in the perception of vibrotactile stimuli proposed that the detection threshold of a mechanical stimulus could be that amplitude at which any activity can be observed in an afferent fiber (LaMotte and Mountcastle, 1975). If it is so, and there exists a correlate in SI with the amplitude of a stimulus, then it would be expected that an increase in cortical activity could be detected for stimuli at a level near 5.60mN. However, during the course of this study, no detectable increase in cortical activity could be discerned for any stimuli of less than 11.79mN using von Frey filaments. Such a threshold is within the observed range of values of the original studies (<0.06-14mN) (Leem et al., 1993a), but it is considered elevated and thus indicative that values reported in the literature were not appropriate for use here. Isoflurane, the primary anesthetic used in this study, is known to increase the firing threshold of cortical neurons in the rat hippocampus and human neocortex (Berg-Johnsen and Langmoen, 1990), so that is likely the cause of the elevation seen.

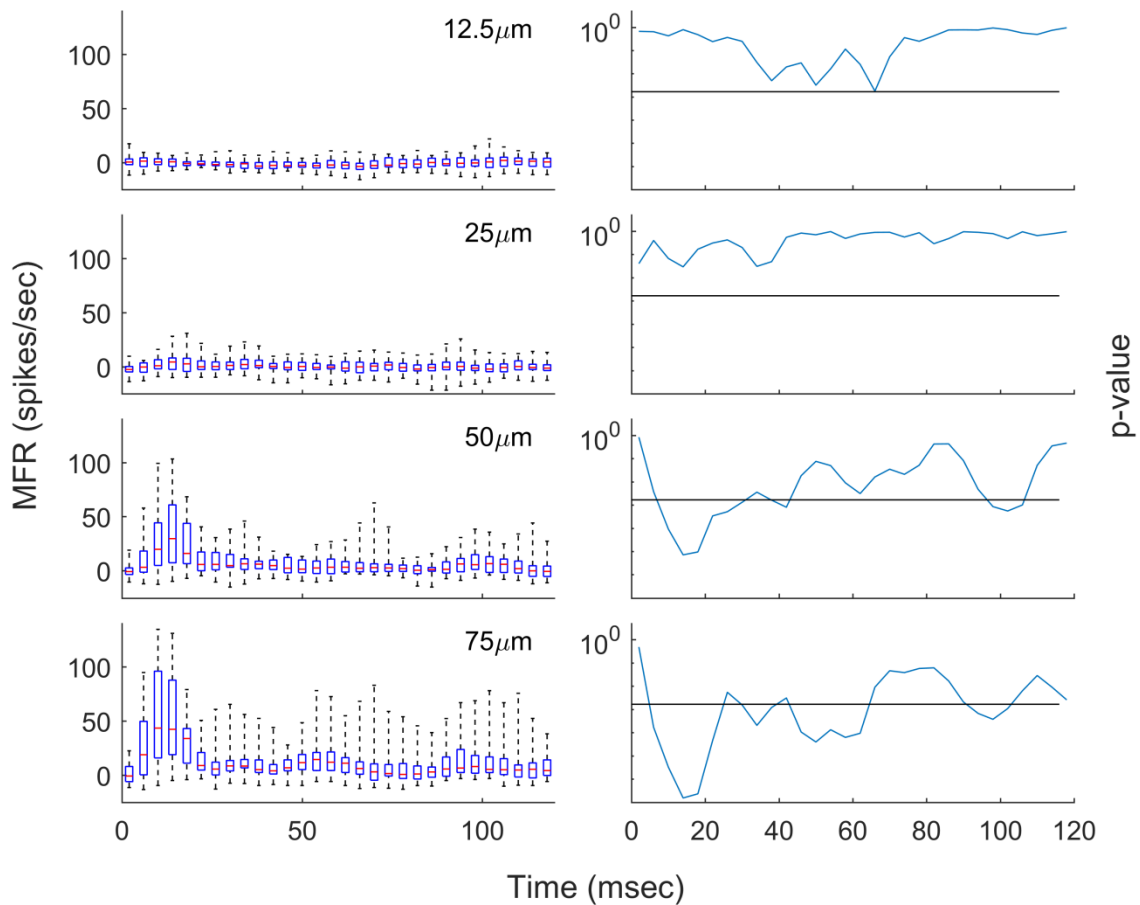


**Figure 2.4: Distribution of Responses with Low-Amplitude Stimulation (All amplitudes peak-to-peak. Black lines represent  $p$ -critical [0.05 with a Bonferroni correction].)**

Therefore, to evaluate Steven's Power Law in this study, it became necessary to empirically determine an appropriate detection threshold (in the chosen units) using the cortical responses collected. The left column of Fig. 2.4 shows the distribution of responses at all recording sites to low-amplitude stimulation of the digit best corresponding to each site's minimal RF (stimulation at the principal digit) over the first 120ms of stimulation. Each box gives the median, 25th and 75th percentiles, and range of observed values across all recording sites (each recording site had its background activity subtracted, then it was scaled by the average number of neurons per recording site, arranged into 4ms bins, and smoothed with a moving weighted average). The right column of the same figure shows  $p$ -values resulting from two-tailed Student's  $t$ -tests performed at each bin

determining if the mean of the distribution was significantly different from zero. The black line represents  $p$ -threshold, where  $p$ -threshold is 0.05 with a Bonferroni correction; the distribution is considered significantly different from background if the  $p$ -value at that bin is below  $p$ -threshold. Prior to each t-test, the distribution at the tested bin was determined to approximate a normal distribution through a Kolmogorov–Smirnov (KS) test ( $p > p$ -threshold).

Firstly, the distributions at 50 and 75 $\mu$ m show significant patterns in a manner consistent with 25Hz-stimulation. At approximately 40ms intervals, there is evidence of an increase in group response that displays some level of significance, though the group response becomes less prominent with extended stimulation. Both amplitudes also display a clear, significant increase in the group response during the first 40ms of stimulation, corresponding to the startle response, and the reduction of subsequent peaks is consistent with adaptation. It is clear that both of these amplitudes evoke a response in a significant portion of the neuron population, and they should be considered suprathreshold.

Next, the distributions at 12.5 $\mu$ m show no clear increase in activity at any point during stimulation. There is no apparent positive response to stimulation, and at some points it could be argued that there is a negative response, suggesting a negative response. However the  $p$ -values resulting from t-tests of the distribution of values at each point are never low enough to reject the null hypothesis. Therefore, 12.5 $\mu$ m should be considered subthreshold.

Lastly, the distributions at 25 $\mu$ m give conflicting information. On one hand, at no point during stimulation is the distribution of values significantly different from background, and that implies that the stimulus is subthreshold. However, during the first 40ms of stimulation there is an increase in the values of individual recording sites, showing that some number of neurons do increase their firing rate at that amplitude. Aspects of this can also be seen the average response in Fig. 2.1. The number of neurons firing is small in comparison to the population, resulting in a

distribution that is not significantly different from the background, but that would be expected with neuron recruitment: a small stimulus would recruit only the most sensitive of neurons. Therefore, if stimulus detection occurs with any increase in activity at the cortical level (caused by a minute increase in activity at the peripheral level), then the detection threshold under these experimental conditions is likely just below  $25\mu\text{m}$ . For the purposes of calculation, it will be assumed from here that the appropriate detection threshold is approximately  $20\mu\text{m}$ , which would be most consistent with this information. Interestingly, this corresponds with the minimum level of stimulation at which entrainment could be seen in rat RA afferent fibers in previous studies (Leem et al., 1993b), but as the cause in threshold elevation in this case is believed to occur at the cortical level, it is likely a coincidence.

This work posited that stimulus amplitude is conveyed at the cortical level through the OMFR of neurons within a macrocolumn over a certain period of time. If such a representation is the means by which relative amplitude is perceived, then according to Steven's Power Law there should exist a power relationship between stimulus amplitude and OMFR with an exponent value around 0.95. Figs. 2.5 and 2.6 evaluate that hypothesis, showing the average increases in cortical response to single-digit stimulation over 120ms for amplitudes above the detection threshold ( $20\mu\text{m}$ ). Such a stimulus duration would likely best reflect the response of the cortex to stimulus amplitude, as the above analysis suggests that cortical activity is heavily modified through temporal dynamics beyond that point (see Section 2.2). Despite technically being above the observed detection threshold, the value for the  $25\mu\text{m}$  stimulus is not shown; this is because the cumulative distribution of the observed recording sites for that amplitude was not significantly different from background activity levels (see Fig. 2.4). The average background activity prior to stimulation has been removed for each amplitude.

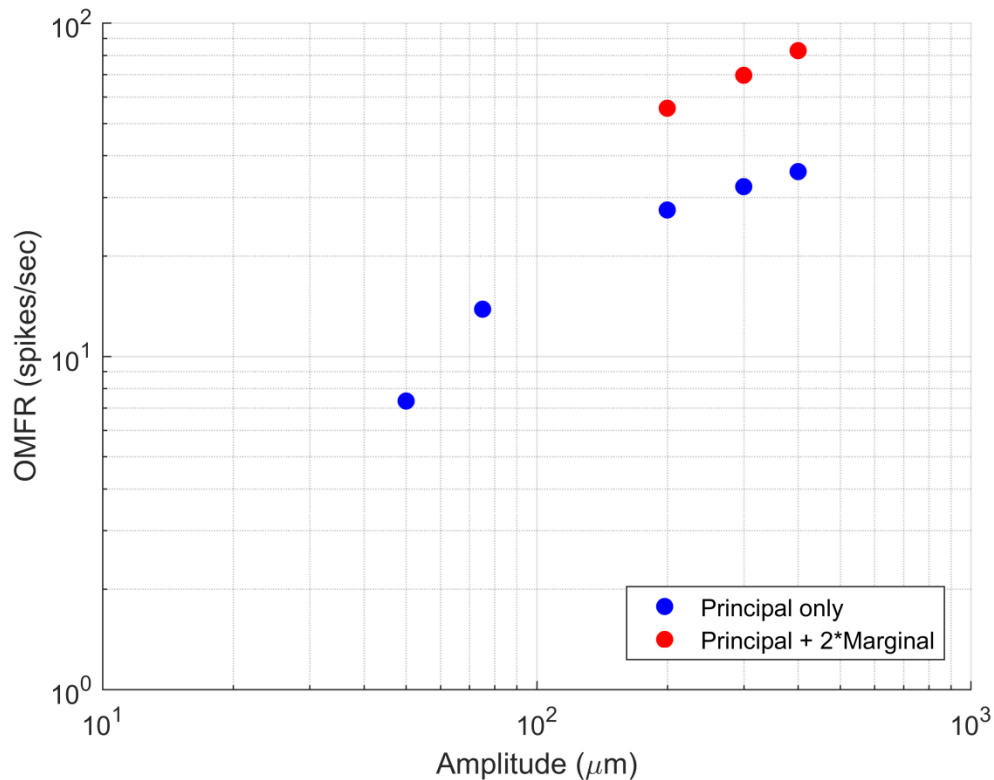


**Figure 2.5: Combined Macrocolumn Responses at Suprathreshold Amplitudes (All amplitudes in  $\mu\text{m}$ , peak-to-peak)**

The OMFR of the single macrocolumn corresponding to the principal digit is shown in blue in Fig. 2.5. Though it does increase with stimulus amplitude as expected, that increase appears to be piecewise, with low amplitudes reflecting one relationship and high amplitudes reflecting another. These results are consistent with the theory proposed in Section 2.2 that low and high amplitude stimuli are expressed through in modalities at the cortex; the switch between the two would occur in the region of  $100\mu\text{m}$ . However, the perception of stimulus amplitude has been reported as being continuous, not piecewise as such data for a single macrocolumn would suggest. Treating the observed amplitudes as a continuum and applying a shift corresponding to the detection threshold, the exponent calculated for the power law relationship for a single macrocolumn shown in Fig. 2.6 (blue) is 0.61. Despite the strength of the closeness of fit of the data to a power law curve ( $R^2=0.97$ ),

such an exponential value is grossly different from the 0.95 value reported in perceptual studies (Stevens, 1959; Talbot et al., 1968). Therefore, the OMFR of a single macrocolumn cannot be the means by which relative amplitude is perceived.

Instead, we propose here that the amplitude of an isolated stimulus is conveyed at the cortical level not just by the OMFR of a single macrocolumn, but by the combined OMFR of all macrocolumns activated during stimulation. The results discussed in Section 2.3 illustrate that during the initial period of stimulation, regions of the cortex not corresponding to that directly stimulated are also activated; this level of activation is more pronounced at higher amplitudes. While such regions may become inactive with time in accordance with the funneling response (Simons et al., 2005, 2007; Tommerdahl et al., 2010), this initial lateral spread suggests they could have an impact on the perception of stimulus amplitude, especially for those greater than  $\sim 100\mu\text{m}$ .

Fig. 2.5 includes estimates of the combined OMFRs of the regions likely activated through single-digit stimulation. The estimates were made by combining the activity of observed macrocolumn when its principal digit was stimulated with twice the activity seen when its marginal digit was stimulated; such an estimate would approximate the activity seen at the directly stimulated macrocolumn as well as those corresponding to adjacent digits (for example, the combined activity of macrocolumns corresponding to digit 3 as well as digits 2 and 4). This activity pattern would reflect a mirrored pattern in the initial lateral spread. No new estimates were made for low-amplitude stimuli, as their low levels of activation in the principal macrocolumn suggest that they would promote a minimal level of activity in adjacent macrocolumns, if any.

The estimates of the high-amplitude stimuli using multiple macrocolumns in Fig. 2.5 (red) appear to better reflect the relationship seen in low-amplitude stimuli than those of a single macrocolumn. The estimates also form a power law relationship with the lower-amplitude stimuli that has a better fit ( $R^2=0.99$ ) than the single-macrocolumn values, as shown in Fig. 2.6 (red). It

would appear that to continue the trends set at low-amplitude stimuli, it is necessary for the cortex to expand the extent of the activated cortical region; as it is believed that each macrocolumn in rat SI is most strongly activated by a single digit, so this expansion is most likely originates at the cortex.

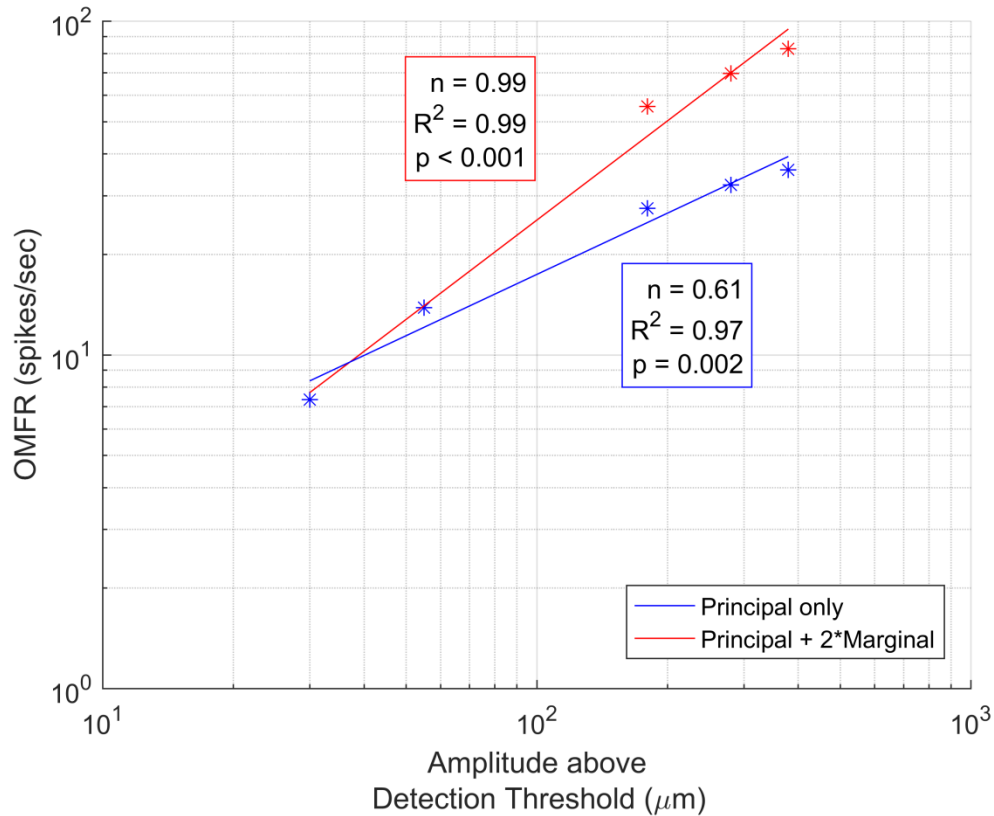


**Figure 2.6: Representation of Stimulus Amplitude at Cortical Level**  
**(All amplitudes in  $\mu\text{m}$ , peak-to-peak, shifted by detection threshold.)**

It is more important to note, however, that the power law relationship formed using the estimated activity of multiple macrocolumns closely matches the expected curve for perception. The exponent calculated for the power law relationship is 0.99, which more closely matches the expected 0.95 value reported in early studies (Stevens, 1959; Talbot et al., 1968). While this model is only an estimate, it does clearly indicate that the amplitude of a single, isolated stimulus is

expressed across an increased expanse of cortex, and the size of the expanse is related to the perception of the stimulus.

Therefore, it can be concluded from these analyses that the amplitude of a flutter vibrotactile stimulus at the periphery is conveyed at the cortical level through the overall mean firing rate of activated macrocolumns. The initial spread of activation can cover multiple adjacent macrocolumns, and the perception of the amplitude at a single stimulus site is directly related to the average activity of the entire region activated.

### **CHAPTER 3: RESPONSES TO SIMULTANEOUS TWO-DIGIT STIMULATION**

Chapter 2 analyzed the effects of single-digit vibrotactile stimulation, and the results supported the hypothesis that the amplitude of a single stimulus applied at the periphery is largely represented in the cortex in the cortical area's overall mean firing rate (OMFR). Given this information, Chapter 3 will investigate the effects of simultaneous two-digit stimulation on cortical activity. Two-digit stimulation involves the co-processing of multiple, near-adjacent macrocolumns for an extended period, and thus it is subject to additional cortical dynamics to which single-digit stimulation is not. These new dynamics, which will be probed through the use of conditioning stimuli, are anticipated to have differential impacts on the cortical response to stimulation at multiple peripheral sites, and by consequence the perception thereof.

The stimulus pattern for two-digit stimulation consists of applying the test stimulus (300 $\mu$ m) to the one digit and the standard stimulus (200 $\mu$ m) to an adjacent digit. In this study, digits 2 and 3 are used; the digit where the minimal receptive field (RF) of the recording site is located is termed the principal digit, and the adjacent digit is termed marginal digit. As a general rule and unless otherwise specified, the test stimulus is applied to the principal digit of the recording site, and thus macrocolumn, under observation, and the standard stimulus is applied to the marginal digit. Since the setup used did not allow for simultaneous recording of macrocolumns, to examine the effects of stimulation as described above at a recording site in an adjacent macrocolumn, stimulus amplitudes were switched such that the test amplitude was applied at the marginal digit relative to the recording site (see Chapter 1). In this way, concurrent activity in two separate macrocolumns could be observed.

In this chapter, terminology relating to activity at the principal and marginal digit locations refers to the macrocolumns to which those digits most strongly project, as discussed in Chapters 1 and 2. All data utilized in statistical tests were first confirmed to follow normal distributions using Kolmogorov–Smirnov (KS) tests ( $p > 0.05$  or  $p$ -threshold), and all t-tests and KS tests involving multiple time points utilized a value  $p$ -threshold for significance testing, where  $p$ -threshold was 0.05 with a Bonferroni correction. Unless otherwise noted, all stimulus amplitudes are in  $\mu\text{m}$  peak-to-peak.

### **Section 3.1 - Single vs. Two-Digit Stimulation**

In Chapter 2, it was discussed that a single vibrotactile stimulus of sufficient amplitude at the periphery could not only evoke activity in the macrocolumn most closely associated with the stimulus site, but also in those that were physically or perhaps functionally adjacent to it. This increase of activity in an adjacent cortical region was attributed to the initial phase of the funneling response, a response having spatial and temporal components which is theorized to result from secondary horizontal communications between macrocolumns and pericolumnar inhibition (Tommerdahl et al., 2010). However, the responses reported in Chapter 2 at adjacent macrocolumns occurred in the absence of stimuli at corresponding digits; it is unclear how such secondary intercommunications will impact cortical activity in the presence of primary afferent drive.

To examine this, Fig. 3.1 gives the average overall mean firing rates (OMFRs) of two adjacent macrocolumns during single or two-digit stimulation; stimulation lasted 500ms, and each activity pattern has been averaged into 40ms (one cycle) bins and smoothed with a moving weighted average. During two-site stimulation, the test stimulus was applied at the principal digit, and the standard stimulus was applied at the marginal digit. As previously described, the response for each

macrocolumn was made by varying the digit to which the test amplitude was applied during simultaneous two-digit stimulation; the digit to which the test stimulus was applied relative to the recording site's minimal RF determined the macrocolumn's designation for that test. To compare the responses of the principal and marginal macrocolumns to their responses to the same stimulus amplitudes but in isolation, single stimuli with amplitudes matching the test and standard stimuli respectively were applied in a single-digit manner to the principal digit relative to the recording site.

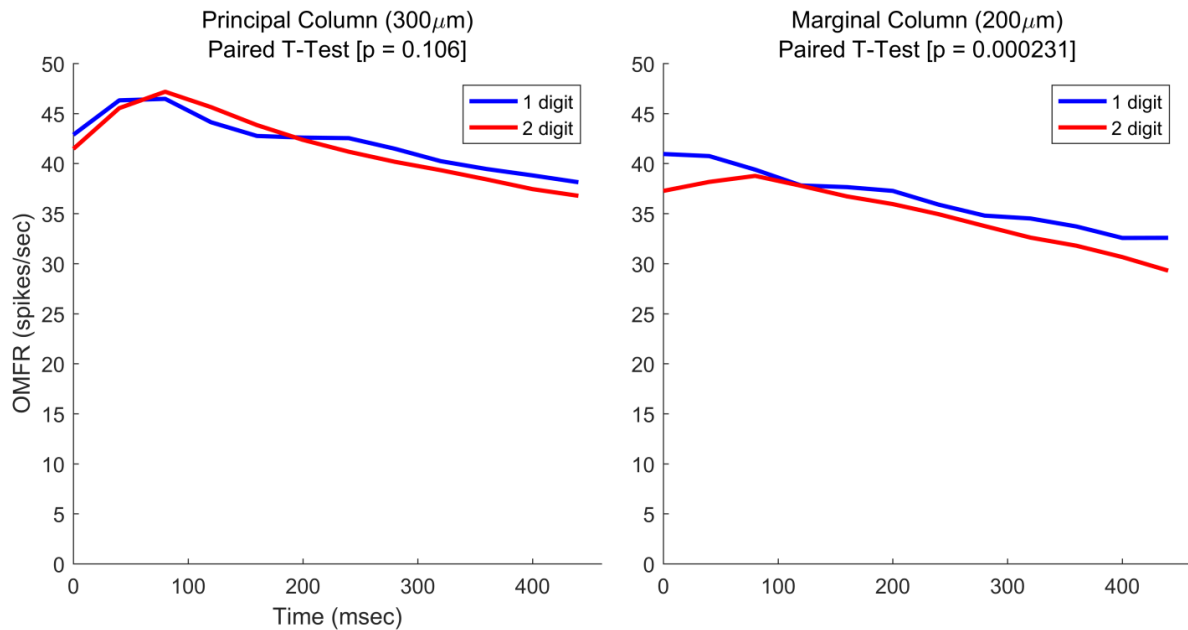


**Figure 3.1: Macrocolumn Responses to Stimulation at 1 or 2 Digits  
 (All amplitudes are µm peak-to-peak)**

The left column of Fig. 3.1 gives the responses of the principal macrocolumn when the test stimulus is applied in isolation and as part of a two-digit stimulus pattern. The responses appear largely similar, suggesting that in this scenario the addition of a second adjacent stimulus does not affect cortical function. A paired t-test between the responses supports this theory, having a  $p$ -value is greater than 0.05. In contrast, the right column of Fig. 3.1 suggests that response of the marginal macrocolumn was slightly, but significantly, reduced through two-digit stimulation. The right column of Fig. 3.2 compares the response of a macrocolumn when the standard stimulus is

applied in isolation and as part of two-digit stimulus pattern, and it is apparent that the macrocolumn is less active during two-digit stimulation. The  $p$ -value of an accompanying paired t-test is below 0.05, indicating that the difference in activity is significant. This differential effect on one macrocolumn but not the other supports the hypothesis that there are spatial aspects in two-digit stimulation that are not present in single-digit stimulation.

The reason for the decrease at the marginal macrocolumn is likely related to the relative amplitude of the stimulus applied at the marginal digit relative to that at the principal digit. A perceptual phenomenon has been previously reported wherein a strong stimulus would reduce sensitivity to other stimuli at adjacent skin regions (von Békésy, 1965). If the OMFR of a cortical region is related to the perception of a stimulus at the same mapped region of the skin, then the results in Fig. 3.1 support the theory that such reduced sensitivity arises at the cortical level, with the region activated by the lesser stimulus being modified by the region activated by the stronger stimulus. This phenomenon is known as lateral inhibition, and it likely results from long-range inhibitory connections between related macrocolumns (Tommerdahl et al., 2010). However, it is unclear if this reduction is directly related to the funneling phenomenon, as the lateral inhibition present occurs during a shorter stimulus, while that explicitly observed in the funneling phenomenon is expected to develop over an extended duration (Simons et al., 2007).

Relatedly, Fig. 3.2 investigates the possibility that activity seen at the marginal macrocolumn during two-digit stimulation is directly caused by the initial spread of the funneling phenomenon. The figure shows the activity at the marginal macrocolumn during single-digit stimulation at the principal digit and during two-digit stimulation. There is a clear increase in activity during two-digit stimulation, and a paired t-test affirms that the increase is significant ( $p < 0.01$ ). Based on this, it can be said that the macrocolumn corresponding to the marginal digit will on average experience an increase in activity during two-digit stimulation over that resulting from stimulation of the principal

digit. This result matches expectations, as primary afferent drive should logically have a greater excitatory effect on cortical activity than indirect connections between macrocolumns, which are believed to be the cause of the funneling phenomenon's initial spread.

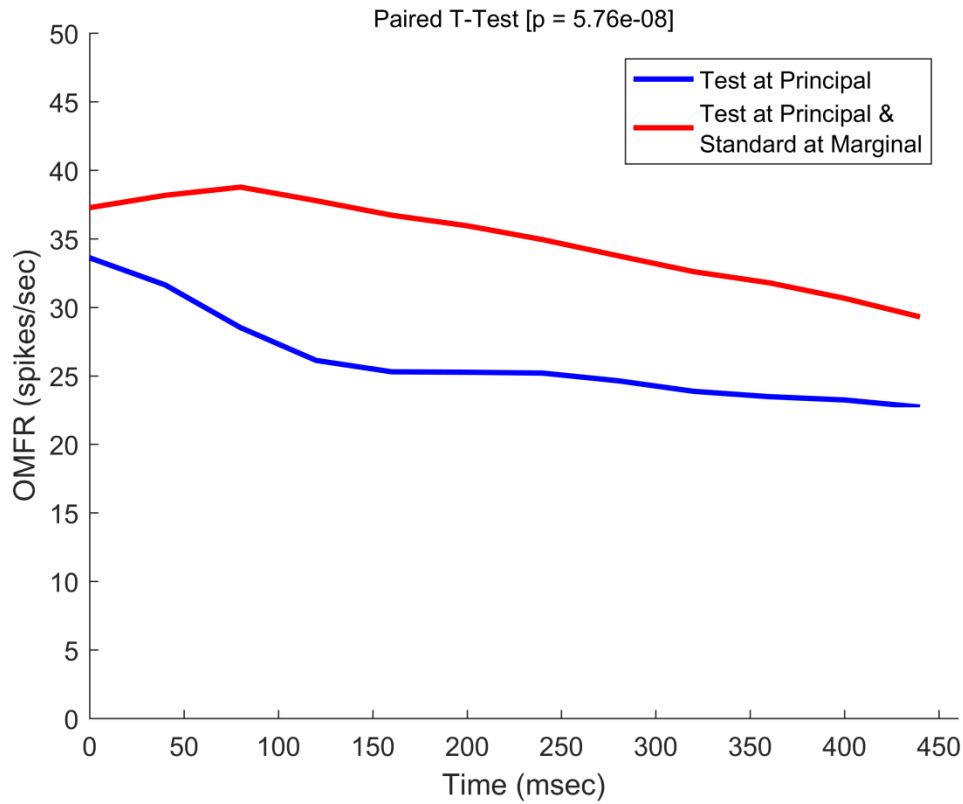


**Figure 3.2: Marginal Macrocolumn Response to Principal Digit and Two-Digit Stimulation**

That said, one test subject displayed remarkably different results in the marginal macrocolumn from the average shown in Fig. 3.2. For that subject [data not shown], two-digit stimulation using test and standard stimuli of 200 $\mu$ m and 100 $\mu$ m respectively resulted in a reduction in activity at the marginal macrocolumn relative to that caused by single-digit stimulation at the principal digit. This is in direct contrast to the increase in activity shown in Fig. 3.2. Though it is possible that the difference in response was caused by the increase in relative difference between the test and standard stimuli, which was 2x as opposed to 1.5x, the singular occurrence of this trend

suggests that the difference is statistical in nature; while individual cells may experience a decrease in activity, in aggregate the marginal macrocolumn will experience an increase.

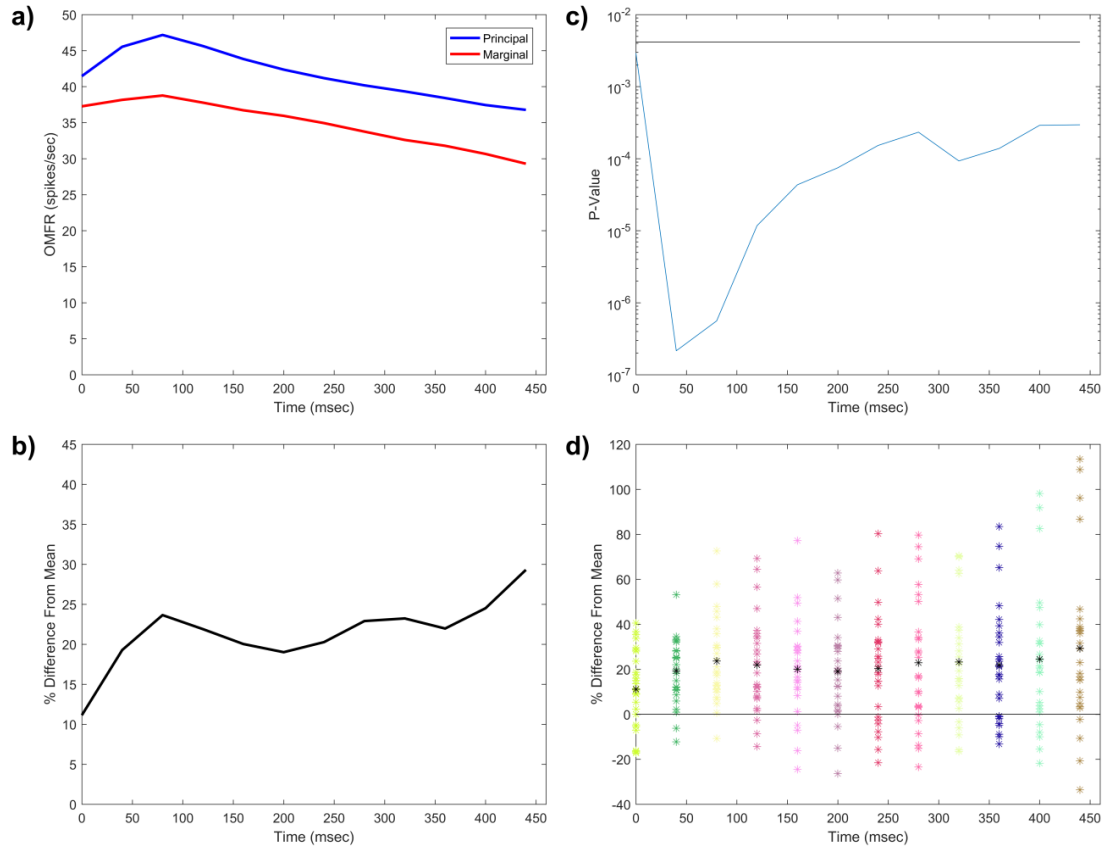


**Figure 3.3: Digit Macrocolumn Responses to Two-Digit Stimulation (Differences are Principal - Marginal)**

To begin evaluating the relative effects of simultaneous two-digit stimulation in adjacent macrocolumns, it is necessary to observe their responses to stimulation relative to one another. Towards this end, the average OMFRs of neurons within adjacent macrocolumns during two-digit stimulation are given in Fig. 3.3a for comparison. It is immediately apparent that the principal macrocolumn, or that to which the principal digit most strongly projects to, has a greater OMFR than that at the marginal macrocolumn, or that corresponding to the marginal digit, at all time

points during stimulation. This suggests that the relative relationship between the digits is preserved, with the more strongly stimulated digit displaying on average higher levels of activity. The two waveforms are significantly different from one another, as confirmed by a paired samples t-test ( $p \ll 0.01$ ).

To examine if the relationship between the two waveforms changed over time, the difference between the response of the principal and marginal macrocolumns scaled against their average response was evaluated for each cycle. For each recording site, the difference between the waveforms from their average was calculated, scaled by the average number of neurons over all recording sites, and smoothed with a moving weighted average. Fig. 3.3d shows the distribution of calculated values, and the averages at each time point are shown in Fig. 3.3b. A series of Student's t-tests shown in Fig. 3.3c confirmed that the distribution of recording site responses was significant for each cycle of stimulation ( $p < p$ -threshold)

Fig. 3.3b shows that the average difference from the mean is initially low, but it progressively rises in subsequent cycles. The initial similarity in values mimics that of the startle response discussed in Chapter 2 wherein the first cycle of stimulation was largely equivalent for all stimulations above approximately 100  $\mu\text{m}$ . Meanwhile, the progressive increase in values is likely related to the differential effects of two-digit stimulation shown in Fig. 3.1, and it suggests that such differential effects develop with extended stimulation. If the OMFR at a macrocolumn corresponding to a single digit is the indicator used to determine the relative magnitude of stimulation at that digit versus another at a perceptual level, then one's ability to discern the difference in stimulation levels between two digits would be relatively weak during early stimulation but would improve with time.

## Section 3.2 - Effects of Single-Site Conditioning

To examine the effects of adaptation due to extended neuron firing, a high-amplitude conditioning stimulus (400 $\mu$ m, 1 sec) was applied to the principal digit prior to two-digit stimulation, with a 500ms gap in between. Adaptation is the phenomenon wherein the responsivity of a neuron or cortical area drops with sustained activity (Whitsel et al., 2003), and it would be expected that such a stimulus would dramatically reduce the ability of the principal macrocolumn to respond to stimulation.

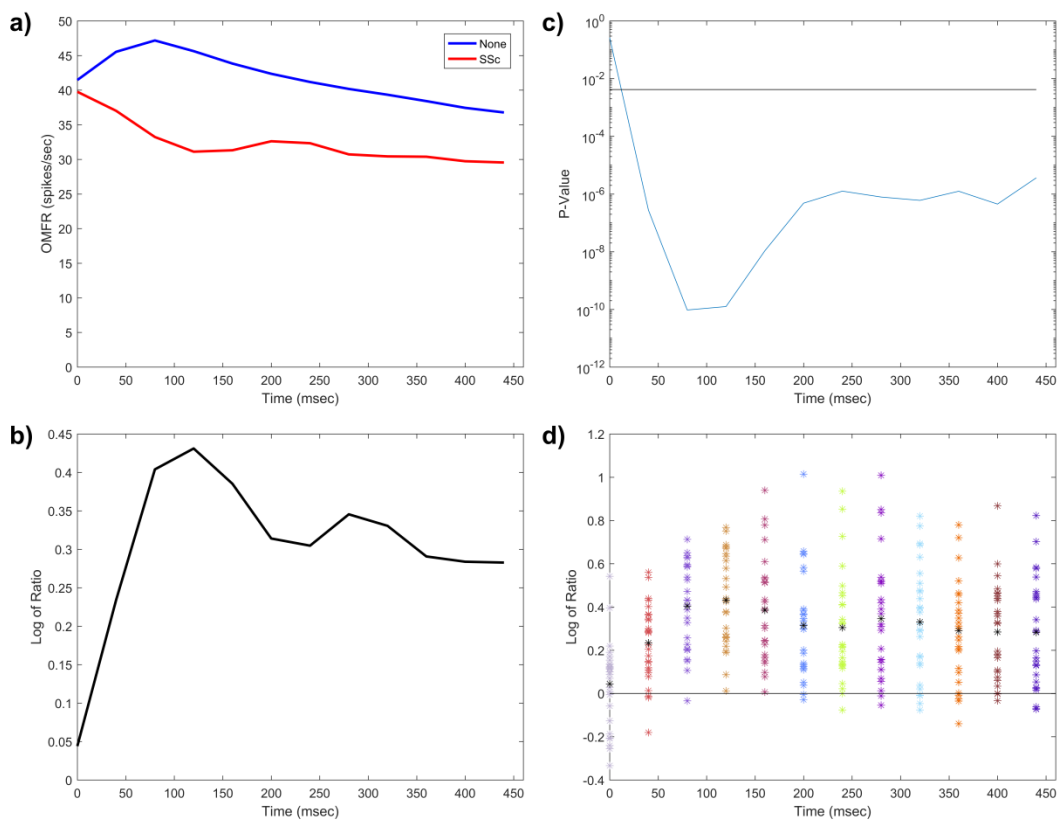


**Figure 3.4: Principal Macrocolumn Response Following Single-Site Conditioning (Ratios are No Conditioning/SSc)**

As predicted, the conditioning stimulus applied to only one digit, termed single-site conditioning (SSc), dramatically reduced the activity seen at the principal digit. The effects of SSc

are shown in Fig. 3.4a as the red line, with the blue line being the activity of the principal macrocolumn during two-digit stimulation without a conditioning stimulus ("None"). Both OMFRs were calculated according to steps given above, and they were determined to be significantly different from one another using a paired samples t-test ( $p \ll 0.01$ ). The reduction in overall activity following SSc suggests the conditioning stimulus caused a change in cortical conditions prior to two-digit stimulation, preventing observed neurons from reacting the same way to the same stimulation. This further indicates that the activity of the cortex is subject to alteration through temporal effects in addition to spatial.

To observe the degree to which cortical activity was altered by SSc, the ratio of cortical activity after SSc and without conditioning was calculated during each cycle of stimulation for each recording site, using similar pretreatment to that previously described. The natural log of these had a broad but normal distribution at each cycle as shown in Fig. 3.4c, but their means, shown in Fig. 3.4b, indicate that on average the activity of the cortex was reduced following SSc.

There are three noteworthy phenomena in the mean log-ratios of the responses that occur in sequence: an initial equivalence, a sharp increase, and a slow decrease. The initial equivalence is likely related to the startle response; it's interesting to see that it remains even following SSc. The sharp increase tells that the difference in activity of the two waveforms widens following the initial cycle; according to the hypothesis that OMFR is related to perception of magnitude, this would indicate that the stimulus becomes perceptually different during that stage. In the same vein, the slow downward slope of the means during remaining cycles implies that the two stimuli become more similar again with time. This could be because the effects of SSc have worn off, or more likely the observed cortical region reaches the same level of adaptation, almost an adaptation plateau, following extended stimulation regardless of the presence of conditioning. However, Student's t-tests performed using the log-ratio of the two stimulus patterns at each time point, shown in Fig.

3.4c, indicate that the two waveforms remain different from each other even through the last cycle of stimulation ( $p < p$ -threshold). The log-ratio of recording site distributions during the first cycle of stimulation is not significantly different from zero, suggesting that the mechanisms behind the startle response are not affected by this type of conditioning.

### Section 3.3 - Effects of Dual-Site Conditioning

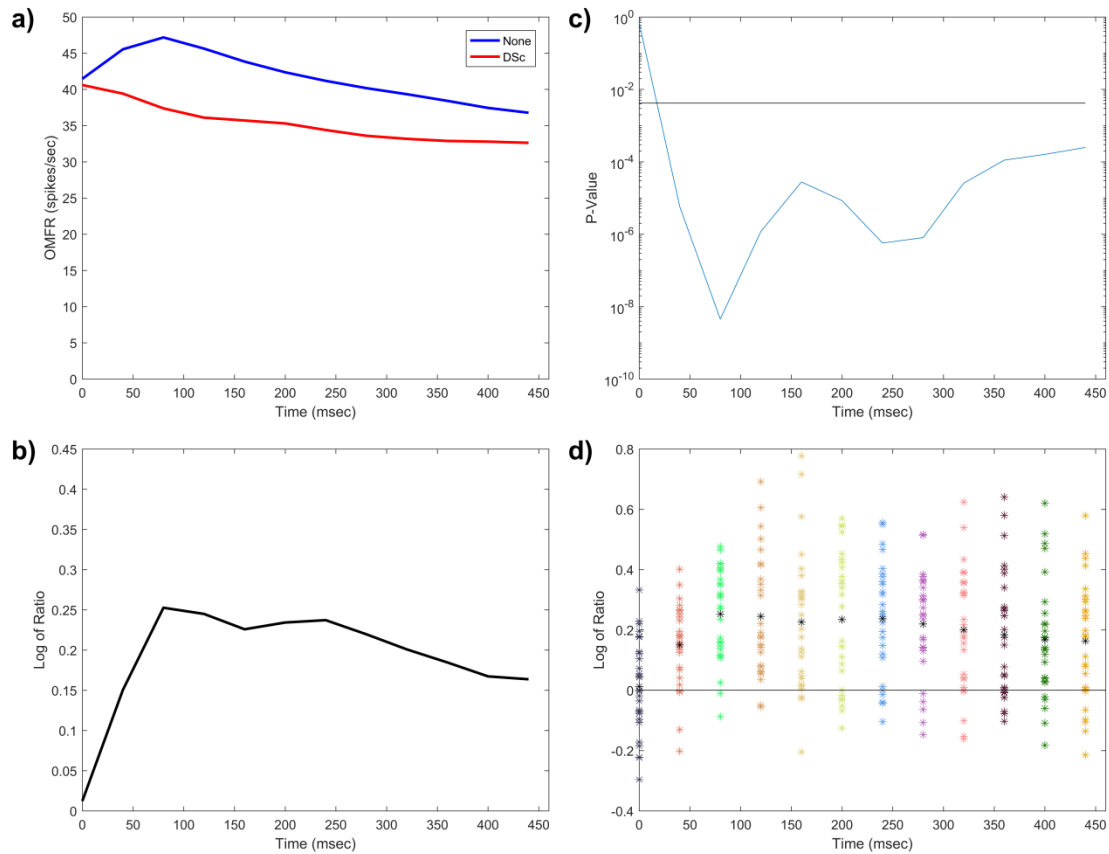


**Figure 3.5: Principal Macrocolumn Response Following Dual-Site Conditioning (Ratios are No Conditioning/DSc)**

SSc stimuli were designed to desensitize a portion of the cortex by effectively extending the period of adaptation for neurons therein. In actuality, it likely also invokes the funneling response, and lateral inhibition, at a single location; the macrocolumn whose receptive field most strongly

corresponds to the conditioned region displays reduced activity through adaptation, while the activity of adjacent, off-center macrocolumns likely display a greater reduction in comparison due to lateral inhibition. However, behaviorally speaking, funneling responses seldom occur in isolation. Rather, activity in the cortex would be expected to be the result of multiple funneling responses of adjacent regions occurring simultaneously. To date, the effects of multiple, separate funneling responses on cortical activity in the somatosensory cortex have not been directly studied.

To evoke such funneling responses and to test the effects of lateral inhibition resulting from two active areas, both digits used in this study were preconditioned with identical, low intensity stimuli (200  $\mu$ m, 1 sec) prior to two-digit stimulation, with a 500ms gap in between. The effects of such a stimulus pattern, termed dual-site conditioning (DSc), are shown in Fig. 3.5a at the principal macrocolumn. The OMFR following DSc was less than that without conditioning for all time points beyond the first cycle, and this difference was shown to be significant through a paired samples t-test ( $p \ll 0.01$ ). This result resembles that seen following SSc, adding further evidence that conditioning of any sort will change the conditions of the cortex prior to two-digit stimulation.

Additional similarities to SSc are seen in the log-ratio of conditioned responses to those without conditioning, as given in Fig. 3.5d and 3.5b. The log-ratios of the activity measured at each recording site increased following the first cycle then slowly fell again as stimulation continued. Despite the similarity in overall trends to SSc, it is interesting to note that the log-ratio of the two stimulation patterns in this case remains virtually equivalent for almost half of the stimulation period. The response to two-digit stimulation following DSc does not begin to meaningfully fall until 250-300 ms into stimulation. Additionally, the log-ratios resulting from DSc are closer to zero than those for SSA (0.2 vs 0.3), indicating that the cortex's activity is reduced to a lesser degree following DSc. Still, a Student's t-test performed during each cycle of two-digit stimulation confirmed that DSc had an impact on cortical function for all stimulus cycles beyond the first ( $p < p$ -threshold).

The tests performed here with SSc and DSc stimuli highlight the temporal effects of conditioning on the cortex. These temporal effects, related to the cortex's funneling phenomenon, appear similar when the principal macrocolumn is examined alone. At the principal macrocolumn, responses following SSc and DSc both considerably reduce cortical response to the same stimulation, and both slowly drift back towards the unconditioned response with time. That said, the primary difference in responses between these conditioning patterns would be more expected to lie in their spatial properties: how the presence or absence of a conditioning stimulus on the marginal digit itself would affect its subsequent response to two-digit stimulation. A single funneling phenomenon should disproportionately affect cortical areas surrounding the receptive field center (Simons et al., 2007), so comparing changes in the marginal digit to those in the principal digit would better highlight differences in cortical response to SSc and DSc.

Fig. 3.6a shows the mean responses to two-digit stimulation following DSc as seen at the principal and marginal macrocolumns. The response at the principal digit is greater than that of the marginal digit for the full duration of stimulation, indicating that on average the difference in stimulus magnitudes at the two locations still produces a difference in OMFR despite DSc. The mean responses were significantly different according to a paired samples t-test ( $p \ll 0.01$ ).

Though the gross difference in stimulation magnitudes appears to be preserved following DSc, the average differences from the mean for each recording site communicate that over time, the responses of the principal and marginal macrocolumns diverge. Following an initial similarity, the average difference from the mean between the two digits appears in Fig. 3.6b and 3.6d to have a positive correlation with increased stimulus duration. Fig. 3.6c shows that such differences were statistically significant for all cycles of stimulation (Student's t-test,  $p < p$ -threshold). The divergence of digits at the end of stimulation (~45%) is greater than that of the response without conditioning reported in Fig. 3.3 (~30%). This suggests that if differences in OMFR is the means from which the

perception of relative stimulus magnitude arises, then the application of DSc prior to two-digit stimulation would likely improve one's ability to discern the larger of the two simultaneous stimuli, even if perception of the actual magnitudes of the stimuli are lost in the process.

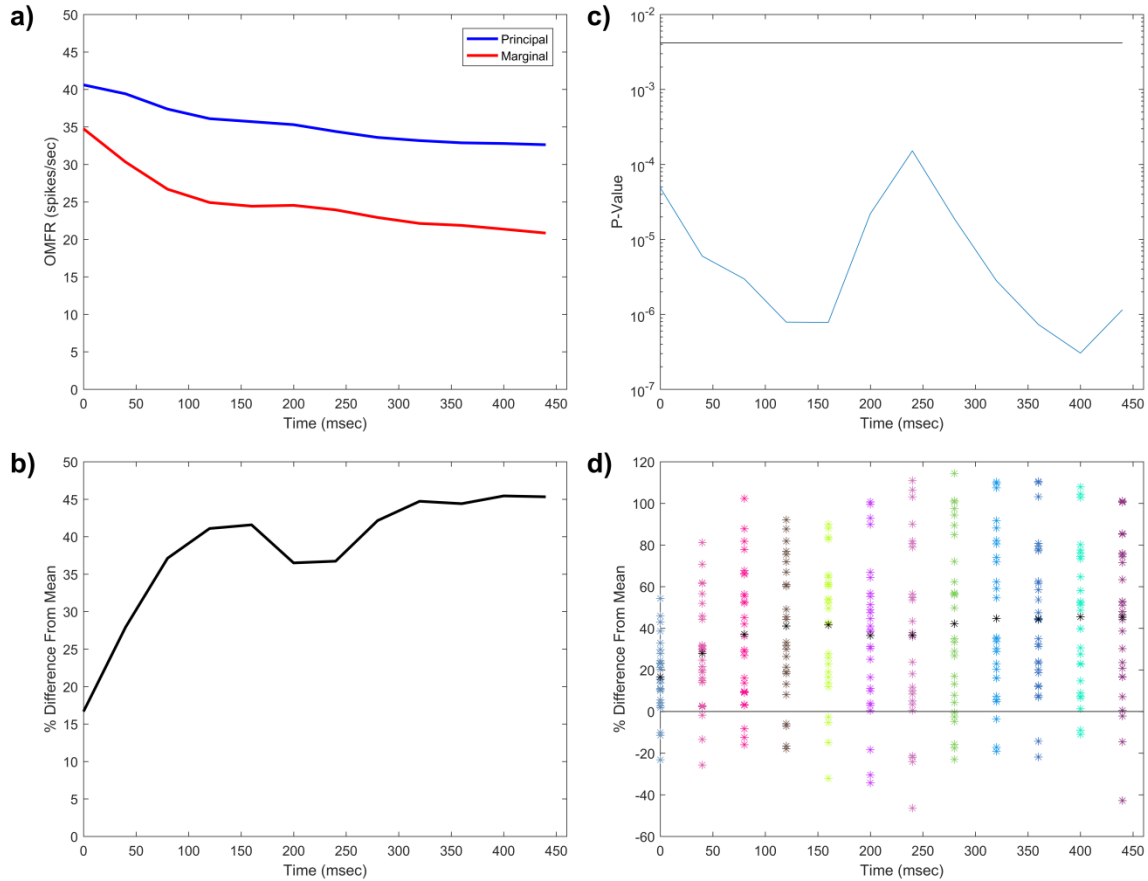


**Figure 3.6: Digit Macrocolumn Responses Following Dual-Site Adaptation (Differences are Principal - Marginal)**

Visual inspection of the mean firing patterns of the principal and marginal digits provides a possible source for the divergence of the digits. In Fig. 3.6a, the marginal digit shows a sharp drop in OMFR following the first cycle, while the principal digit instead has a gentler slope downwards. While further analysis would need to be done to confirm the significance of this trend, it suggests that the difference between the digits following DSc arises primarily from changes occurring at the

marginal digit, rather than the principal. This hypothesis is further supported by the previous observation that while the cortical representation of the principal digit is initially reduced following DSc, it gradually approaches the activity seen at the principal digit without conditioning (see Fig. 3.5a).

### Section 3.4 - Impact of Conditioning on Amplitude Discrimination

Here it has been shown that the responses of macrocolumns servicing two digits become more different with time following DSc. In human perceptual studies, DSc has been shown to improve subjects' ability to discern the larger of two stimuli as compared to without conditioning (Tannan et al., 2007). Therefore, it is likely that this ability, termed amplitude discrimination (AD) is likely related to this differential change in activity between digit macrocolumns. If that is the case, then further insight into this hypothesis could be gained through the comparison of metrics similar to those discussed above between digit macrocolumns with and without conditioning.

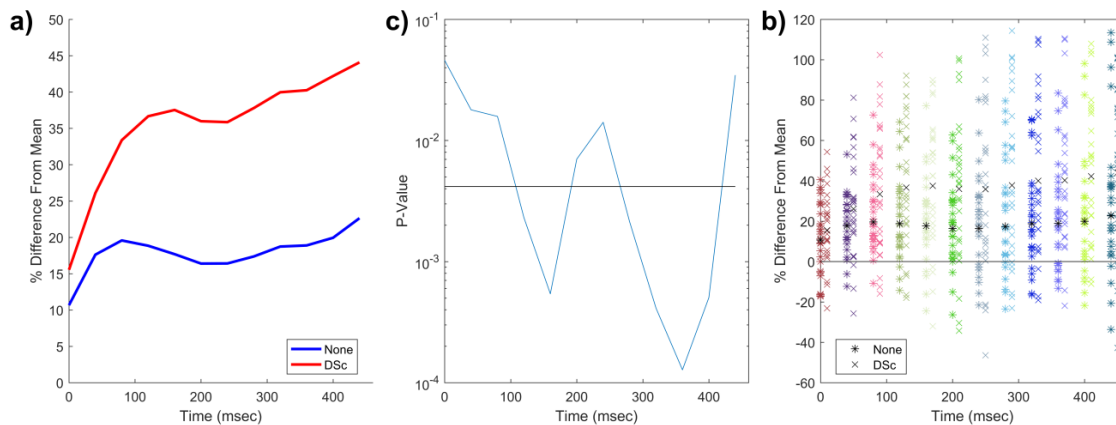


**Figure 3.7: Time Courses as Source of Amplitude Discrimination Performance**

Results of one such comparison are given in Fig. 3.7. Fig. 3.7a shows the average of differences relative to the mean for two-digit stimulation without conditioning and following DSc.

As expected, the two average waveforms were significantly different from one another (paired t-test,  $p \ll 0.01$ ), and their time courses are visibly different from one another.

However, the series of paired t-tests performed at each cycle of stimulation using the values calculated for all penetrations, as shown in Fig. 3.7b, contradict this result. Comparing on a site-by-site basis, there are a number of cycles during which the difference between the responses of the principal and marginal digits relative to their average value for stimulation without conditioning and following DSc was not significant ( $p > p$ -threshold). Those are not sequential, and they show no clear trend. The penetration values shown in Fig. 3.7c also do not appear to support the difference with and without conditioning, as at each time point the distributions of values for the two test patterns appear similar to one another. These results suggest that differences in the OMFR of stimulated regions are not the modality through which AD performance arises.

A second modality for AD that can be tested is the ratio of OMFR of the regions stimulated. Amplitude Discriminatory ability follows Weber's law in healthy subjects (Francisco et al., 2008), which makes the ratio of the magnitudes of applied stimuli the determining factor when discerning differences in amplitude at the perceptual level. From this, it stands to reason that such a phenomenon may be seen in the somatosensory cortex. Despite this, tests comparing the log-ratio of the OMFR of the principal and marginal macrocolumns showed results virtually equivalent to those above; the log-ratio was not significantly different when conditioning was applied. In this regard, neither the difference nor the ratio between cortical regions appears to be a viable candidate for the source of AD performance, at least not for any given recording site. Therefore, it is likely that only in aggregate can the change in activity at both the principal and marginal macrocolumns produced through DSc be the cause for the reported improvement in AD performance.

As such, the mean cortical responses of the principal and marginal digits for two-digit stimulation following each style of conditioning (None, SSc, and DSc) are presented together in Fig. 3.8a. Viewed in this manner, the responses at the principal and marginal digit locations to multiple stimulus patterns can be more directly compared.

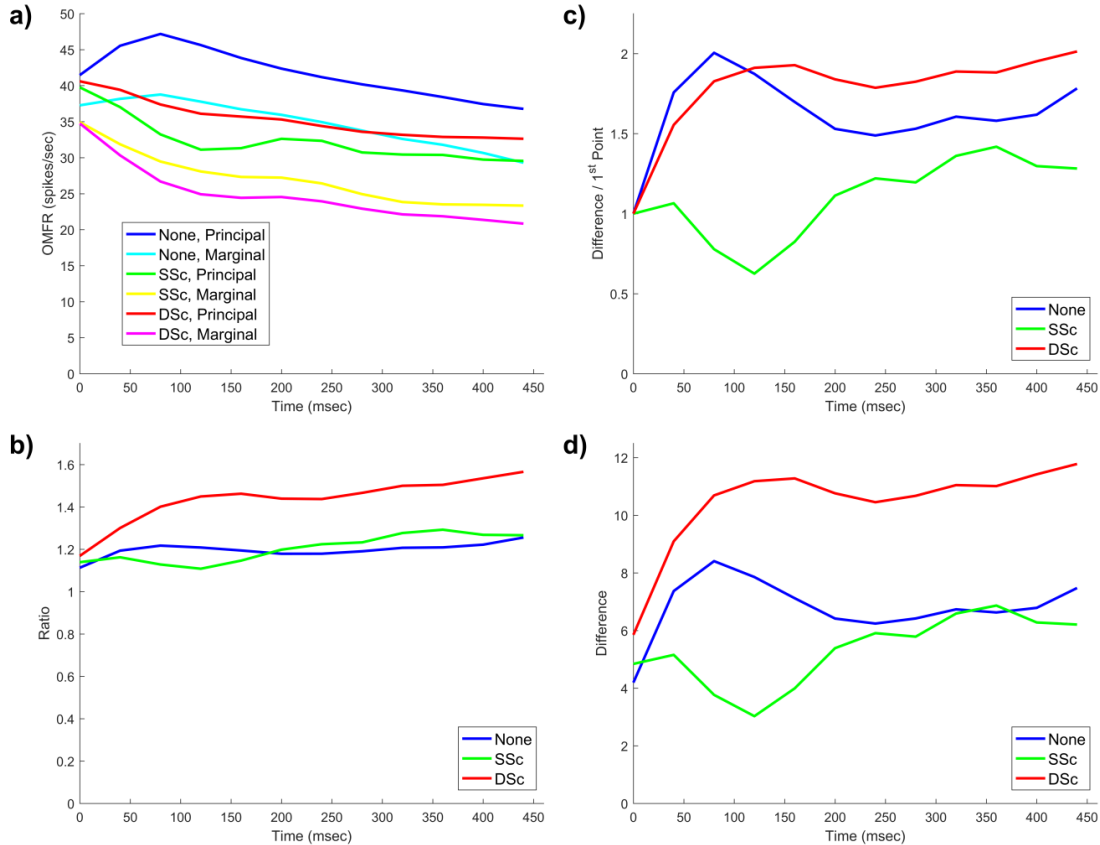


**Figure 3.8: Macrocolumn Comparisons for Amplitude Discrimination**

Firstly, note that for all tests and spatial relations the cortical responses are initially high but trend downwards with increased stimulus duration. This is similar to the effects of adaptation discussed in Chapter 2. That it occurs at both the principal and marginal digits for all conditioning variations suggests that conditioning primarily affects the initial conditions in which adaptation occurs, rather than prevents its occurrence. The high initial activity in each test presumably

corresponds to the startle response. The distribution of initial values appears to be bimodal, where the responses seen at the principal digit are distributed around a different, higher mean than those seen at the marginal digit for all conditioning variations. This, and the observation in Chapter 2 showing that single-digit startle responses are largely equivalent above a certain stimulus amplitude, suggests that the startle response is largely unaffected by conditioning but is instead dependent on observed location.

Next, it is evident that following conditioning, the cortical representations of both the principal and marginal digit experience a large drop in overall activity compared to those without conditioning. This effect was partially investigated previously for the principal digit in Sections 3.2 and 3.3, but here it is obvious that the effect occurs at the marginal digit as well. The reason for these drops must be related to the presence of conditioning and its evoking of one or more funneling responses with lateral inhibition, though the effect on a given region will vary. For example, those sites whose corresponding digits were stimulated during conditioning may still be experiencing some reduction in activity resulting from adaptation, while those sites whose corresponding digits received no such stimulation would be more greatly affected by secondary aspects of the funneling response, such as the previously-reported suppression of adjacent cortical regions (Simons et al, 2007).

In addition to the overall difference in activity levels, a clear difference can be seen between the responses without conditioning and those with conditioning during the first 3-4 cycles of two-digit stimulation. During that period, both locations without conditioning show an increase above initial values before trending downwards; as discussed previously in Chapter 2, this is likely related to the entrainment phenomenon of individual neurons that arises following extended stimulation. In contrast, no responses following conditioning stimuli exhibit such a rise, instead only decreasing during that period. Given that the out-of-phase peaks that precede entrainment only occur early in

stimulation, it is possible that the recorded neurons became entrained during conditioning and remained so at the time of two-digit stimulation. Observations made using the same data averaged into 4ms bins [data not shown] support this hypothesis, as noteworthy out-of-phase peaks occur early in conditioning but are largely unseen or of reduced magnitude during the two-digit stimulation period. This entrainment effect is another temporal phenomenon through which conditioning affects cortical responses, and it may have other implications to perception that are not directly investigated in this study, such as frequency discrimination (Whitsel et al., 2001; Tommerdahl et al., 2005) or temporal order judgment (Tommerdahl et al., 2007) .

Finally, it is interesting to note that while the responses at the principal digit are visibly different between SSc and DSc, the responses seen at the marginal macrocolumn following conditioning are largely equivalent. This is an unexpected result, given that the marginal digit was only directly manipulated during DSc but not SSc. It raises the possibility that both on and off-center conditioning will both bring about the same response to a lesser stimulus if an adjacent region is stimulated more strongly. However, it is more likely a coincidence, with SSA affecting the region prior to stimulation through added suppression and DSA affecting the region through increased adaptation. The similarity of the effects on cortical activity seen here is likely unique, resulting from the choices in the conditioning stimuli magnitudes utilized in this study.

Fig. 3.8b investigates the hypothesis that the ratio of responses seen at the principal macrocolumn relative to those seen at the marginal macrocolumn are responsible for AD performance. For each conditioning variant, the ratio of the mean response seen at the principal macrocolumn relative to that seen at the marginal macrocolumn is plotted against time, suggesting how much greater the perception of the stimulus at the former may seem relative to the latter. Firstly, it can be seen that the ratio of responses without any conditioning rises initially, following the initial similarity due to startle response, drops, then gradually climbs back upwards. This

suggests that if the ratio of responses is the means through which AD operates, then AD performance without conditioning should be greatest in the first few hundred milliseconds of two-digit stimulation, become worse for a time, then gradually improve once again.

The initial peak is likely related to the conclusion in Chapter 2 that the cortical representation of amplitude is most accurate early in stimulation, before adaptation, entrainment, and other dynamic effects can develop. In that light, the difference in responses is purely that of the cortical responses to amplitudes of different amplitudes. The drop then would be a result of differences in adaptation between regions, with the area more strongly stimulated potentially experiencing a faster drop in activity. The final, subsequent rise would best highlight the effects of pericolumnar lateral inhibition and the funneling phenomenon, as their continued influence on the contrast between affected regions would become more prominent with time. It would be expected that this upward trend would occur with or without conditioning, as it is likely more dependent on concurrent stimulation than initial activity levels.

In comparison, the ratio of responses following DSc in Fig. 3.8b shows a similar pattern to that seen without conditioning, but with higher contrast. Following an initial similar response during the first cycle (startle response), the ratio of responses is seen to be far greater following DSc, indicating a much greater relative difference in response at the cortical representations of the two digits. If the ratio of responses is utilized in AD, then DSc would likely result in an improvement of AD performance. This result echoes those in human perceptual studies (Tannan et al., 2007). As with without conditioning, the activities of the digits' cortical representations become less similar with time, which would likely lead to even greater improvements in AD performance with increased stimulus duration.

Unexpectedly, the ratio of responses following SSc in Fig. 3.8b do not follow a single trend as those of the other conditioning variants. Following the initial, similar response, the ratio of

responses following SSc drops during the few hundreds of milliseconds of stimulation. The ratios within this range are well below those without conditioning, indicating that the responses stemming from the principal and marginal digits are more similar following SSc. In human perceptual studies, SSc worsens AD performance in healthy subjects (Tannan et al., 2007); if the ratio of responses is the mechanism from which AD performance arises, then the two results agree with one another during early stimulation. However, after a few hundred milliseconds, the ratio of responses rises above those seen without conditioning, indicating that the responses of the two digits become more different with time. This does not match perceptual studies; subjects' discriminatory abilities were tested at the end of a 500ms two-digit stimulation pattern, which according to these results should result in an improvement in AD performance. Therefore, it seems unlikely that the ratio of responses between two stimulated regions is the mechanism that gives rise to AD performance.

Fig. 3.8c and 3.8d investigate an alternative hypothesis: AD performance is related to the difference in responses seen at the principal macrocolumn relative to those seen at the marginal macrocolumn. Fig. 3.8c scales the difference in responses by the difference during the first cycle of stimulation, while Fig. 3.8d does not include any type of scaling. In both the scaled and unscaled versions, the difference of responses following SSc are in general less than those without conditioning. This more appropriately matches perceptual studies, and, combined with Fig. 3.8a, it leads to the conclusion that SSc causes a reduction in activity at both digit representations as well as an overall reduction in the difference between said digits.

Where the use of scaling for the difference of responses has an impact is in the interpretation of DSc results. As mentioned previously, it has been shown that DSc improves AD performance in healthy subjects (Tannan et al., 2007). As these tests examined subjects' discriminatory ability at the end of a 500ms two-digit stimulus, and both versions of the difference of responses show a greater final difference following DSc than without conditioning, both

interpretations of the cortical response seem plausible. However, given that the gradual upward slope in both (technically all three) time courses is supposedly due to an increase in contrast from lateral inhibitory effects, and DSc's stimulation of both digits could hypothetically be starting the mechanisms driving lateral inhibition earlier, it is more likely that the unscaled version is more accurate. If DSc does prime lateral inhibition prior to two-digit stimulation, then it would have difference values uniformly higher than those without conditioning, and that is shown in Fig. 3.8d.

These results, paired with the previous conclusions regarding the representation of amplitude in the cortex, strongly support the theory that the worsening of AD performance following SSc and the improvement of AD performance following DSc can be explained through changes in relative OMFRs. Therefore, the difference in stimulus amplitude at the perceptual level is most likely related to the total difference in OMFR between the two stimulated regions during the stimulation period.

## **CHAPTER 4: REDUCTION OF CORTICAL ACTIVITY THROUGH DYNAMIC STIMULATION**

In Chapters 2 and 3, all of the tests performed utilized vibrotactile stimuli that should be considered static. Though it is the nature of vibrotactile stimuli to oscillate about a point, the amplitude of the oscillations applied were always the same for a given test condition; the 300 $\mu$ m test stimulus consisted of a sine wave that was 300 $\mu$ m peak-to-peak from start to finish. In this regard, as the stimulus itself is held constant, and the responsiveness of afferent fibers innervating cortical neurons is largely considered to remain constant over time, any changes seen in the cortical response to a sustained, suprathreshold, static stimulus would be expected to result from the cortical activity itself. Similar to the way holding a static load progressively fatigues the muscles supporting that load, the firing of excitatory neurons itself affects neurons' ability to fire. Spatiotemporal dynamics such as adaptation, entrainment, and the early and late phases of the funneling response discussed in Chapters 2 and 3 are prime examples of such cortical activity-driven changes.

However, certain cells present in the cortex have properties that suggest there are other dynamics that can alter the cortical response at amplitudes below those that would normally promote activity. Such cells, specifically neurogliaform (NGF) and basket cells, release inhibitory neurotransmitters in a manner that, with the correct stimulus, would induce a slow, progressive inhibition of cortical neurons, reducing their sensitivity to normally suprathreshold stimuli (Tamás et al., 2003; Oláh et al., 2009; for reviews, see Miller et al., 2001 and Overstreet-Wadiche and McBain, 2015). In this chapter, the effects of such desensitization, termed feed-forward inhibition (FFI), will be examined at the cortical level through the use of a unique stimulus pattern that increases slowly

from sub- to suprathreshold levels, and the potential impact of such effects on the perception of vibrotactile stimuli will be discussed.

#### **Section 4.1 - Neurological Basis for Feed-Forward Inhibition**

Believed to be integral to the signal processing and linearization functions of input layer neurons (Favorov and Kursun, 2011), NGF cells are interneurons that release the inhibitory neurotransmitter  $\gamma$ -Aminobutyric acid (GABA) in a spatially-diffuse, non-specific manner (Oláh et al., 2009). NGF cells release GABA into the intercellular space, as opposed to directly at a postsynaptic terminal, which promotes the binding of GABA to extrasynaptic GABA<sub>A</sub> and GABA<sub>B</sub> receptors. While such neurotransmitter release would allow a single NGF cell to impact the excitability of multiple neurons within a local area, the distance between the release site and receptors would increase the time from release to the onset of inhibition. This, combined with the slower, longer lasting inhibitory post-synaptic potentials (IPSPs) produced by GABA<sub>B</sub> receptors (Tamás et al., 2003), leads to the belief that inhibition caused involving NGF cells requires significant time to develop.

The primary excitatory inputs to NGF cells, and GABA<sub>A</sub>-receptor-mediated basket cells which provide more rapid inhibition, comes from thalamic relay neurons (Tamás et al., 2003; Overstreet-Wadiche and McBain, 2015). Those thalamic neurons, which relay information from primary afferent neurons, are same neurons that primarily innervate excitatory neurons in the middle cortical layers, so both excitatory and inhibitory neurons in the middle layers receive the same afferent drive from stimulation at the periphery. Such an arrangement of connections produces feed-forward inhibition (FFI), with thalamocortical drive promoting slow-developing inhibition in those cells it would otherwise excite.

While there is no indication that FFI would not have an impact on the time course of cortical activity during suprathreshold stimulation, a test evaluating the specific impact of FFI in such a

situation would be difficult to design, requiring that other prominent spatiotemporal effects like those examined in Chapters 2 and 3 be somehow nullified. It is even possible, if not likely, that NGF-related FFI is one of multiple cortical mechanisms that produce such effects. Instead, as inhibitory cells are known to be more sensitive to low-amplitude stimulation than excitatory neurons (Kyriazi and Simons, 1993; Kimura et al., 2010; for review, see Miller et al., 2001), the effects of FFI can be better probed using subthreshold stimulation.

Towards this end, tests performed in this chapter induced FFI in local cortical populations through the use of a ramping stimulus. The ramping stimulus, applied at the principal digit (digit 2 or 3) of each recording site at 25Hz, began at 0 $\mu$ m peak-to-peak and slowly increased by 2 $\mu$ m/sec to a maximum amplitude of 80 $\mu$ m. Such stimulation would provide initially sub-threshold afferent drive (see Chapter 2) to activate NGF and basket cells, allow the slower components of inhibition time to develop, then evoke activity in excitatory neurons through suprathreshold afferent drive. If FFI operates as expected, cortical activity at suprathreshold levels should be reduced overall, and it is possible that the threshold at which activity begins would be increased as well.

## **Section 4.2 - Cortical Response to Ramping Stimulation**

The overall mean firing rate (OMFR) of neurons within a single macrocolumn resulting from ramping stimulation is shown in Fig. 4.1. The raw data were collected into 200ms bins, smoothed with a moving weighted average, and the average spontaneous activity measured over the 500ms prior to stimulation was subtracted. An exemplary stimulus waveform is included to show where stimulation started and ended (for illustration's sake, the exemplary stimulus is lower frequency than that applied) . The figure shows that the ramping stimulus elicits cortical activity over multiple stages during, and after, stimulation. Firstly, during the initial stages of stimulation (~0-12sec), the average activity of neurons in the macrocolumn is indistinguishable from spontaneous activity.

Next, during the second stage (~12-18sec), activity appears raised but inconsistent, continuing to fluctuate around spontaneous levels. Subsequently, during the third stage of stimulation (~18-40sec), activity increases slowly with time. Finally, following the end of stimulation, activity drops below spontaneous levels, and it remains there for the remainder of the recorded period (3 sec).

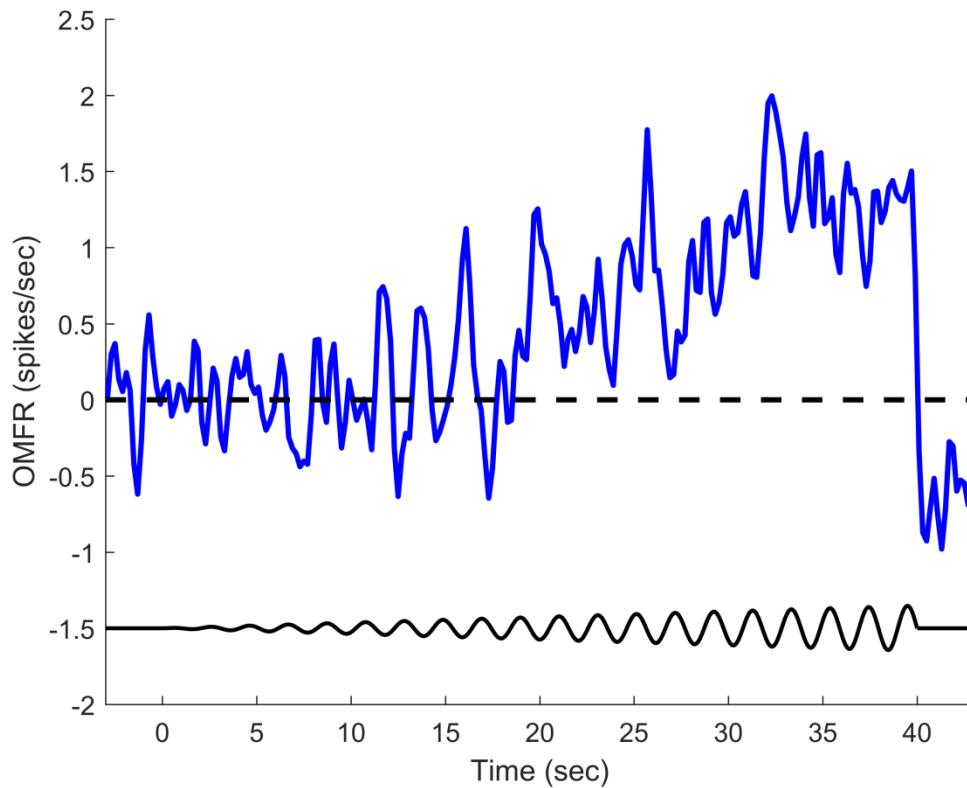


**Figure 4.1: Average Neuron Response with Ramping Stimulation**

From this information, a number of conclusions can be drawn regarding the activity of the macrocolumn. The initial stage of stimulation shows no meaningful change in activity, confirming the assumption that excitatory neurons in the macrocolumn would not be activated by stimuli at low amplitudes delivered in this manner. Results in Chapter 2 with very low amplitude stimuli (12.5 $\mu$ m) further support this claim, and it is during this stage that inhibitory cells are expected to be releasing GABA and applying inhibition to excitatory neurons. The second stage of stimulation is harder to interpret, and it suggests that cortical activity during this period is variable. Appearing

almost periodic, but not being related to stimulus frequency (25Hz), it is possible that such activity reflects momentary increases in activity caused by a tenuous balance of excitation and inhibition, or there may be a range of amplitudes at which some neurons are inhibited while others are not, depending on their proximity to inhibitory cells or the cortical layer in which they reside. Alternately, given the low firing rates seen are still less than 1.5 spikes/second for an average neuron, the trend may simply be noise.

The cortical activity during the third stage of stimulation matches a pattern that would be expected in a stimulus of increasing amplitude. There is a weak but positive correlation in cortical activity with time that is significant ( $R = 0.66$ ,  $R^2=0.43$ ,  $p<0.001$ ), and since the amplitude of the stimulus is increasing during this time, that supports the theory that the average firing rate does still increase with stimulus amplitude despite any FFI present. It is unclear with this information if the activity seen during this period is below that of static stimuli of similar amplitudes, but the final stage of activity strongly suggests that the cortex is heavily inhibited following, and likely during, the ramping stimulus. Spontaneous activity following the ramping stimulus is below pre-stimulus levels, and this indicates that the cortical region as a whole is experiencing a level of depression due to the ramping stimulus. Such an effect was not seen following shorter-duration, high-amplitude static stimulation [data not shown].

Fig. 4.2 shows the distribution of activity seen at different points during stimulation and the results of statistical testing thereon. The data recorded at each recording site were processed as above after scaling each recording site by the average number of neurons over all recording sites (4.5) and sorting the data into 500ms bins. Each box in the top window gives the median, 25th and 75th percentiles, and maximal range of values observed at each time point. For statistical analysis, the distribution of values within each bin was first confirmed to follow a normal distribution through a Kolmogorov–Smirnov (KS) test ( $p>p$ -threshold, where  $p$ -threshold is 0.05 with a Bonferroni

correction). This was followed by a series of two-tailed Student's t-tests to determine if the distribution was significantly different from background levels ( $p < p$ -threshold), and the  $p$ -values for each test are displayed in the bottom window.

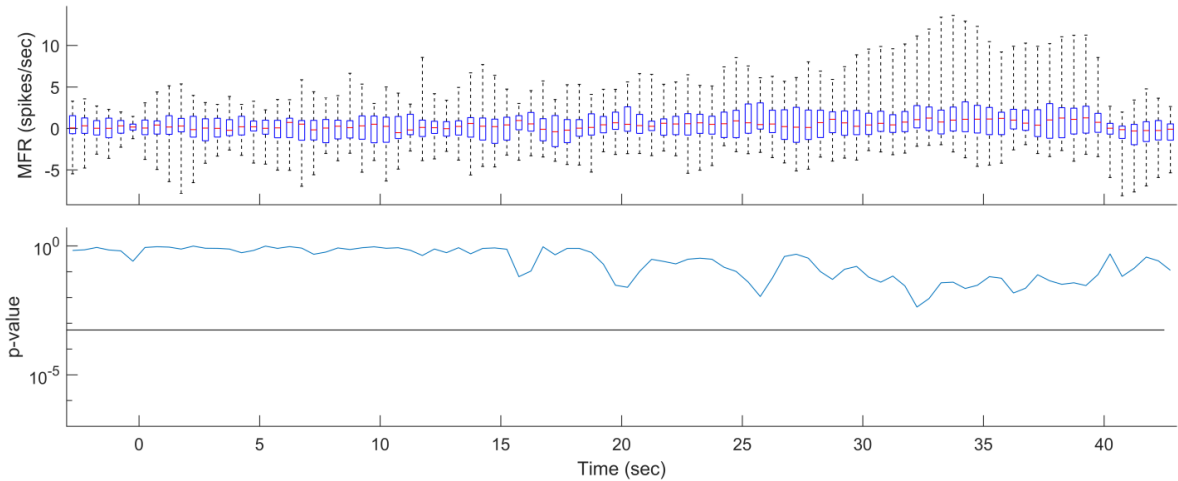


**Figure 4.2: Distribution of Responses with Ramping Stimulation (Black lines represent  $p$ -threshold [0.05 with a Bonferroni correction].)**

The top window in Fig. 4.2 shows that while there may have been a gradual increase in recorded values, the majority of responses appeared to fall within the same low range. Any systematic increase in values was small, though there were some outstanding values at approximately 12 seconds and after 25 seconds of stimulation that could have affected the average displayed in Fig. 4.1. That said, the distribution of values does still appear to drop below background levels after stimulation; this region also appears to have outstanding values that could have affected results in Fig. 4.1.

Far more importantly, however, is that at no point during or after stimulation was the distribution of values significantly different from background firing rates. The  $p$ -values shown in the bottom window of Fig. 4.2 at no point drop below  $p$ -threshold, meaning that the null hypothesis could not be rejected for any portion of the response. This is in direct contrast to the results given in Chapter 2, wherein static stimuli above  $50\mu\text{m}$  produced distributions that were at least at some

portions significantly different from the background. This leads to the conclusion that the ramping stimulus did produce significant inhibition in the cortex, reducing the overall ability of cortical neurons in a macrocolumn to increase their activity in response to a suprathreshold stimulus. Only in aggregate do they display meaningful activity.

### **Section 4.3 - Impact of Feed-Forward Inhibition on Perception**

The responses discussed in Section 4.2 lead to the hypothesis that cortical activity in a macrocolumn would be suppressed by a ramping stimulus, showing only small increases of activity during later stages of stimulation or producing no change in activity at all. However, to draw conclusions on the perception of such activity, it is necessary to compare the activity during a ramping stimulus to that of static stimuli of equivalent amplitude.

Fig. 4.3 compares the effects of a slowly-ramping stimulus on cortical activity against that of static stimuli, and the difference between them is immediately apparent. The data for static stimuli are the same as those given in Chapter 2, taking the OMFR of the first 120ms of stimulation; note that the distribution of values that contributed to the first two points (12.5 and 25 $\mu$ m) were shown to not be statistically significant from background spontaneous levels. The data for the ramping stimulus is arranged into 500ms bins, which corresponds to a 1 $\mu$ m/bin increase in amplitude.

It is clear that the average responses of the cortex during the ramping stimuli, though still increasing, are dramatically lower than those resulting from static stimuli for the range tested. The highest amplitudes delivered through the ramping stimulus elicit a response only slightly higher than those of the lowest amplitudes, and that response is almost a magnitude less than that of a comparable higher amplitude stimulus. Based on these results, it can be said that a ramping stimulus does affect cortical activity, and it promotes inhibition in a temporal manner such that the cortical response to suprathreshold stimuli is greatly reduced.

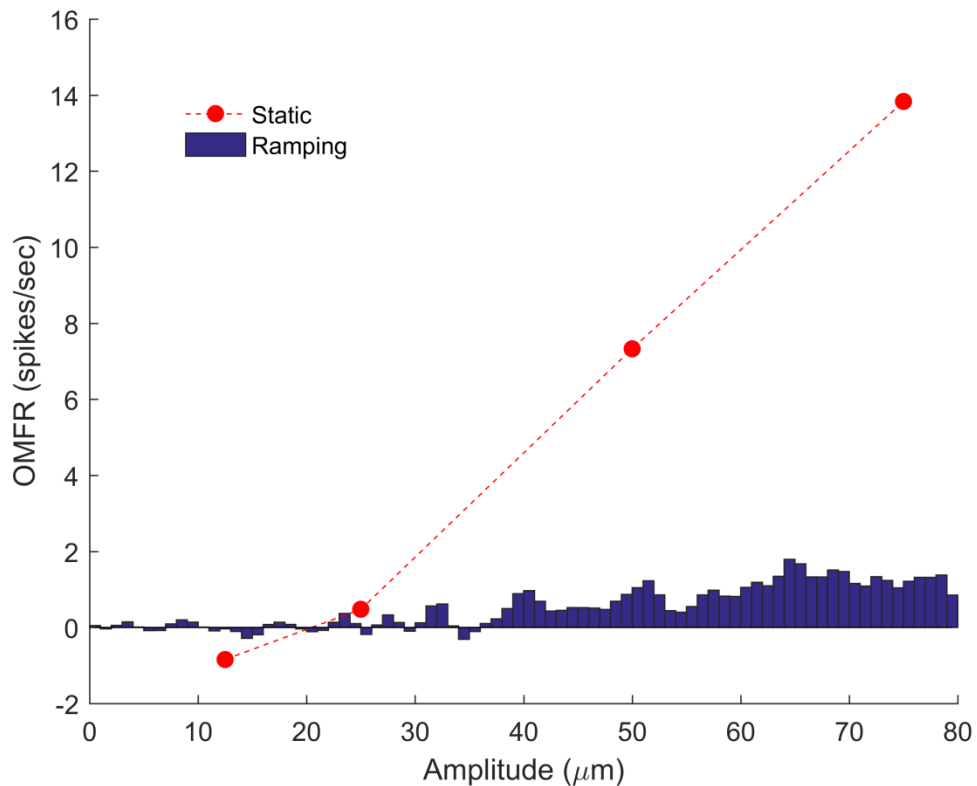


**Figure 4.3: Cortical Response to Static vs. Ramping Stimuli  
(All amplitudes are  $\mu\text{m}$  peak-to-peak)**

In Chapter 2, the hypothesis was proposed that the perception of low-amplitude stimuli is related to the OMFR of neurons within a macrocolumn. As results in both Chapters 2 and 3 supported that hypothesis, the data presented here suggest that stimulus amplitudes delivered in a ramping manner would be felt far less intensely than those delivered in a static manner.

While other tests in Chapter 3 utilizing longer stimuli would support that conclusion, perceptual tests utilizing a ramping stimulus have instead focused on subjects' ability to determine the amplitude at which the stimulus could be detected. This stimulus amplitude was termed the dynamic detection threshold, and in healthy subjects its value was always greater than the static detection threshold found using traditional stimuli (Zhang et al., 2011b). It was theorized that FFI suppressed cortical activity such that a higher amplitude stimulus level was required for subjects to

detect the stimuli. However, based on the approach used in Chapter 2 to estimate the detection threshold of subjects within this study, the results reported here conflict somewhat with that theory. Figs. 4.1 and 4.2 show that the first large spike in activity during ramping stimulation appears to occur at approximately 12 seconds, or  $24\mu\text{m}$ , which is very similar to the level approximated in Chapter 2; this suggests that the effects of the ramping stimulus in this region of the cortex are not responsible for the greater value in the dynamic threshold.

That said, if stimulus detection requires some level of group activity, as opposed to individual neuron spiking as used in Chapter 2, then the results here would likely be consistent with perceptual studies. The overall mean firing rate of neurons in the observed macrocolumn is greatly reduced at all previously suprathreshold amplitudes, so it is likely that activity at the level of the original detection threshold is also reduced. As activity during the ramping stimulus does exhibit a weak positive trend, activity levels approaching those resulting in detection would not occur until the ramping stimulus reached an appropriate, higher amplitude. Additional behavioral studies in rats would be required to discern which method perceptual threshold determination is more appropriate before conclusions could be drawn on this matter.

Alternately, during one series of early analyses [data not shown], there appeared to be a difference in responses to ramping stimuli in neurons in different layers of the cortex. The average response of neurons in the middle layers was similar to in appearance to Fig. 4.3, having a slow increase in activity for amplitudes greater than approximately  $36\mu\text{m}$ , though the activity remained below that observed with static stimuli. In contrast, neurons in the deep cortical layers showed no meaningful increase in activity during the ramping stimulus, remaining at the spontaneous level for the entire duration. Both sets of activity dropped below background levels once the stimulus was stopped. Receiving their inputs directly from afferent neurons in the thalamus, it is generally believed that neurons in the middle cortical layers provide inputs to neurons in other layers of the

same column. If the detection threshold of a stimulus requires firing in layers other than the middle layers, but those layers are more greatly affected by FFI, then this could explain the discrepancy between the results given here and perceptual studies (Zhang et al., 2011b). Further targeted study into this particular issue would likely provide additional insights into not only the function of FFI but into the perceptual means of the detection threshold metric as well.

## CONCLUSIONS

In this study, the spatiotemporal response dynamics in the rat primary somatosensory cortex (SI) were directly studied through the use of standardized vibrotactile stimuli and extracellular recordings of neurons' spike discharges. Numerous other studies have shown that perception of such patterns of tactile stimuli can be sensitive to alterations in the cortical mechanisms that underlie perception, and the work presented here supports their theories regarding the origins of such perceptual changes in healthy subjects.

The first spatiotemporal phenomenon examined was the effect of stimulus amplitude on the cortical response, and it was found that increasing the amplitude of a single stimulus resulted in an increase in activity at the macrocolumn that processes afferent information from the stimulated skin site. Additionally, it was confirmed that the cortical representation of amplitude has a spatial component as well, as a single stimulus promoted activity in multiple cortical columns, including those in which the stimulated region was not part of their minimal receptive field. This observation lead to further analysis into the perception of stimulus amplitude, and it was found that the combined activity of activated cortical columns more closely matched human perception.

The second spatiotemporal phenomenon examined was that of lateral inhibition and adaptation. The results of two-digit stimulation showed that macrocolumns servicing two adjacent stimulus sites were disproportionately affected by stimulation according to their relative amplitudes. The application of a high-amplitude conditioning stimulus to a single site resulted in adaptation in the macrocolumn of the corresponding digit and produced results consistent with a worsening of amplitude discriminatory performance. In comparison, the application of low-

amplitude stimuli to both skin sites resulted in contrast-enhancing differences, producing results consistent with an improvement in amplitude discriminatory ability. Analysis of potential means of amplitude discriminatory ability at the cortical level suggested that the ability arises from the total difference in activity levels in the macrocolumns corresponding to the stimulated skin sites.

The last dynamical phenomenon examined here was feed-forward inhibition (FFI). The ramping stimulus utilized resulted in profound suppression of the cortical response to stimulus amplitude as compared to static stimulation of discrete amplitudes. Such a result is consistent with perceptual studies regarding detection thresholds, assuming that detection occurs when the overall mean firing rate of a macrocolumn surpasses a certain threshold.

The work presented here quantified the operation of SI in healthy, neurotypical subjects. In populations with underlying cortical dysfunction, it has been shown in numerous studies the perception of the same stimuli utilized here is fundamentally changed, resulting in a difference in collected metrics from the neurotypical population. To assist in the study of such neurological disorders, injuries, and alterations, the data analyzed here will serve as a baseline dataset against which similar data collected in atypical populations can be compared. At this time, we are preparing a series of experiments to study these same spatiotemporal dynamics in alcohol-dependent and concussed rats. In performing these experiments and others like them in other neurologically altered populations, we will be able to gain insights into the cortical mechanisms affected by such neurological conditions, and the knowledge obtained will be useful in their monitoring and in the design of treatments.

## REFERENCES

- Berg-Johnsen, J., & Langmoen, I. A. (1990). Mechanisms concerned in the direct effect of isoflurane on rat hippocampal and human neocortical neurons. *Brain Research*, 507(1), 28–34.
- Favorov, O. V, Diamond, M. E., & Whitsel, B. L. (1987). Evidence for a mosaic representation of the body surface in area 3b of the somatic cortex of cat. *Proceedings of the National Academy of Sciences of the United States of America*, 84(18), 6606–6610.
- Favorov, O., & Whitsel, B. L. (1988). Spatial organization of the peripheral input to area 1 cell columns. I. The detection of “segregates”. *Brain Research*, 472(1), 25–42.
- Favorov, O. V, & Diamond, M. E. (1990). Demonstration of Discrete Place Defined Columns - Segregates- in the Cat SI. *The Journal of Comparative Neurology*, 298, 97–112.
- Favorov, O. V, & Kursun, O. (2011). Neocortical layer 4 as a pluripotent function linearizer. *Journal of Neurophysiology*, 105(3), 1342–1360.
- Favorov, O. V, Kursun, O., & Tommerdahl, M. (2017). Role of Feed-Forward Inhibition in Neocortical Information Processing: Implications for Neurological Disorders. In I. Opris & M. F. Casanova (Eds.), *The Physics of the Mind and Brain Disorders* (pp. 383–397). Springer International Publishing.
- Folger, S. E., Tannan, V., Zhang, Z., Holden, J. K., & Tommerdahl, M. (2008). Effects of the N-methyl-D-Aspartate receptor antagonist dextromethorphan on vibrotactile adaptation. *BMC Neuroscience*, 9, 87.
- Francisco, E., Tannan, V., Zhang, Z., Holden, J., & Tommerdahl, M. (2008). Vibrotactile amplitude discrimination capacity parallels magnitude changes in somatosensory cortex and follows Weber’s Law. *Experimental Brain Research*, 191(1), 49–56.
- Johnson, K. O. (1974). Reconstruction of population response to a vibratory stimulus in quickly adapting mechanoreceptive afferent fiber population innervating glabrous skin of the monkey. *Journal of Neurophysiology*, 37(1), 48–72.
- Ketcham, C. J., Hall, E., Bixby, W. R., Vallabhajosula, S., Folger, S. E., Kostek, M. C., ... Patel, K. (2014). A neuroscientific approach to the examination of concussions in student-athletes. *Journal of Visualized Experiments*, (94).
- Kimura, F., Itami, C., Ikezoe, K., Tamura, H., Fujita, I., Yanagawa, Y., ... Ohshima, M. (2010). Fast activation of feedforward inhibitory neurons from thalamic input and its relevance to the regulation of spike sequences in the barrel cortex. *The Journal of Physiology*, 588(5), 2769–2787.
- Kohn, A., & Whitsel, B. L. (2002). Sensory cortical dynamics. *Behavioural Brain Research*, 135(1–2), 119–126.

- Kursun, O., Sakar, B. E., Isenkul, M. E., Sakar, C. O., Gurgun, F., Delil, S., ... Favorov, O. V. (2013). Analysis of Effects of Parkinson's Disease in Somatosensory System via CM-4 Tactile Stimulator. In *International Conference on Applied Informatics for Health and Life Sciences* (pp. 57–60). Istanbul, Turkey.
- Kyriazi, H. T., & Simons, D. J. (1993). Thalamocortical response transformations in simulated whisker barrels. *The Journal of Neuroscience*, *13*(4), 1601–1615.
- LaMotte, R. H., & Mountcastle, V. B. (1975). Capacities of humans and monkeys to discriminate vibratory stimuli of different frequency and amplitude: a correlation between neural events and psychological measurements. *Journal of Neurophysiology*, *38*(3), 539–559.
- Leem, J. W., Willis, W. D., & Chung, J. M. (1993a). Cutaneous sensory receptors in the rat foot. *Journal of Neurophysiology*, *69*(5), 1684–1699.
- Leem, J. W., Willis, W. D., Weller, S. C., & Chung, J. M. (1993b). Differential activation and classification of cutaneous afferents in the rat. *Journal of Neurophysiology*, *70*(6), 2411–2424.
- Miller, K. D., Pinto, D. J., & Simons, D. J. (2001). Processing in layer 4 of the neocortical circuit: new insights from visual and somatosensory cortex. *Current Opinion in Neurobiology*, *11*(4), 488–497.
- Mountcastle, V. B. (1957). Modality and topographic properties of single neurons of cat's somatic sensory cortex. *Journal of Neurophysiology*, *20*(4), 408–434.
- Mountcastle, V. B., Talbot, W. H., Sakata, H., & Hyvarinen, J. (1969). Cortical neuronal mechanisms in flutter-vibration studied in unanesthetized monkeys. Neuronal periodicity and frequency discrimination. *Journal of Neurophysiology*, *32*(3), 452–484.
- Mountcastle, V. B. (1978). An organizing principle for cerebral function: the unit module of the distributed system. In G. M. Edelman & V. B. Mountcastle (Eds.), *The Mindful Brain* (pp. 7–50). Cambridge, MA: MIT Press.
- Nguyen, R. H., Kirsch, B., Yu, R., Shim, S., Mangum, P., Holden, J. K., ... Tommerdahl, M. (2013a). An undergraduate laboratory exercise to study sensory inhibition. *Journal of Undergraduate Neuroscience Education*, *11*(2), A169-73.
- Nguyen, R. H., Gillen, C., Garbutt, J. C., Kampov-Polevoi, A., Holden, J. K., Francisco, E. M., & Tommerdahl, M. (2013b). Centrally-mediated sensory information processing is impacted with increased alcohol consumption in college-aged individuals. *Brain Research*, *1492*, 53–62.
- Nguyen, R. H., Ford, S., Calhoun, A. H., Holden, J. K., Gracely, R. H., & Tommerdahl, M. (2013c). Neurosensory assessments of migraine. *Brain Research*, *1498*, 50–58.
- Oláh, S., Fule, M., Komlosi, G., Varga, C., Baldi, R., Barzo, P., & Tamas, G. (2009). Regulation of cortical microcircuits by unitary GABA-mediated volume transmission. *Nature*, *461*(7268), 1278–1281.

- Overstreet-Wadiche, L., & McBain, C. J. (2015). Neurogliaform cells in cortical circuits. *Nature Reviews. Neuroscience*, *16*(8), 458–468.
- Powell, T. P., & Mountcastle, V. B. (1959). Some aspects of the functional organization of the cortex of the postcentral gyrus of the monkey: a correlation of findings obtained in a single unit analysis with cytoarchitecture. *Bulletin of the Johns Hopkins Hospital*, *105*, 133–162.
- Puts, N. A. J., Edden, R. A. E., Wodka, E. L., Mostofsky, S. H., & Tommerdahl, M. (2013). A vibrotactile behavioral battery for investigating somatosensory processing in children and adults. *Journal of Neuroscience Methods*, *218*(1), 39–47.
- Roldan, C. J., & Abdi, S. (2015). Quantitative sensory testing in pain management. *Pain Management*, *5*(6), 483–491.
- Simons, S. B., Tannan, V., Chiu, J., Favorov, O. V, Whitsel, B. L., & Tommerdahl, M. (2005). Amplitude-dependency of response of SI cortex to flutter stimulation. *BMC Neuroscience*, *6*(43).
- Simons, S. B., Chiu, J., Favorov, O. V, Whitsel, B. L., & Tommerdahl, M. (2007). Duration-dependent response of SI to vibrotactile stimulation in squirrel monkey. *Journal of Neurophysiology*, *97*(3), 2121–2129.
- Stevens, S. S. (1959). Tactile vibration: dynamics of sensory intensity. *Journal of Experimental Psychology*, *57*(4), 210–218.
- Talbot, W. H., Darian-Smith, I., Kornhuber, H. H., & Mountcastle, V. B. (1968). The sense of flutter-vibration: comparison of the human capacity with response patterns of mechanoreceptive afferents from the monkey hand. *Journal of Neurophysiology*, *31*(2), 301–334.
- Tamás, G., Lorincz, A., Simon, A., & Szabadics, J. (2003). Identified sources and targets of slow inhibition in the neocortex. *Science*, *299*(5614), 1902–1905.
- Tannan, V., Simons, S., Dennis, R. G., & Tommerdahl, M. (2007). Effects of adaptation on the capacity to differentiate simultaneously delivered dual-site vibrotactile stimuli. *Brain Research*, *1186*, 164–170.
- Tannan, V., Holden, J. K., Zhang, Z., Baranek, G. T., & Tommerdahl, M. A. (2008). Perceptual metrics of individuals with autism provide evidence for disinhibition. *Autism Research*, *1*(4), 223–230.
- Tavassoli, T., Bellesheim, K., Tommerdahl, M., Holden, J. M., Kolevzon, A., & Buxbaum, J. D. (2016). Altered tactile processing in children with autism spectrum disorder. *Autism Research*, *9*(6), 616–620.
- Tommerdahl, M., Hester, K. D., Felix, E. R., Hollins, M., Favorov, O. V, Quibrera, P. M., & Whitsel, B. L. (2005). Human vibrotactile frequency discriminative capacity after adaptation to 25 Hz or 200 Hz stimulation. *Brain Research*, *1057*(1–2), 1–9.

- Tommerdahl, M., Tannan, V., Zachek, M., Holden, J. K., & Favorov, O. V. (2007). Effects of stimulus-driven synchronization on sensory perception. *Behavioral and Brain Functions*, 3(61).
- Tommerdahl, M., Favorov, O. V., & Whitsel, B. L. (2010). Dynamic representations of the somatosensory cortex. *Neuroscience and Biobehavioral Reviews*, 34(2), 160–170.
- Tommerdahl, M., Dennis, R. G., Francisco, E. M., Holden, J. K., Nguyen, R., & Favorov, O. V. (2016). Neurosensory Assessments of Concussion. *Military Medicine*, 181(5 Suppl), 45–50.
- Verberne, W. R., Snijders, T. J., Liem, K. S., Baakman, A. C., & Veldhuijzen, D. S. (2013). Toepassingen van sensibiliteitsonderzoek met 'quantitative sensory testing'. *Nederlands tijdschrift voor geneeskunde*, 157(5), A5434.
- Von Bekesy, G. (1965). Inhibition and the time and spatial patterns of neural activity in sensory perception. *Transactions of the American Otological Society*, 53, 17–34.
- Waters, R. S., Li, C. X., & McCandlish, C. A. (1995). Relationship between the organization of the forepaw barrel subfield and the representation of the forepaw in layer IV of rat somatosensory cortex. *Experimental Brain Research*, 103(2), 183–197.
- Whitsel, B. L., Kelly, E. F., Delemos, K. A., Xu, M., & Quibrera, P. M. (2000). Stability of rapidly adapting afferent entrainment vs responsivity. *Somatosensory & Motor Research*, 17(1), 13–31.
- Whitsel, B. L., Kelly, E. F., Xu, M., Tommerdahl, M., & Quibrera, M. (2001). Frequency-dependent response of SI RA-class neurons to vibrotactile stimulation of the receptive field. *Somatosensory & Motor Research*, 18(4), 263–285.
- Whitsel, B. L., Kelly, E. F., Quibrera, M., Tommerdahl, M., Li, Y., Favorov, O. V., ... Metz, C. B. (2003). Time-dependence of SI RA neuron response to cutaneous flutter stimulation. *Somatosensory & Motor Research*, 20(1), 45–69.
- Zhang, Z., Zolnoun, D. A., Francisco, E. M., Holden, J. K., Dennis, R. G., & Tommerdahl, M. (2011a). Altered central sensitization in subgroups of women with vulvodynia. *The Clinical Journal of Pain*, 27(9), 755–763.
- Zhang, Z., Francisco, E. M., Holden, J. K., Dennis, R. G., & Tommerdahl, M. (2011b). Somatosensory information processing in the aging population. *Frontiers in Aging Neuroscience*, 3, 18.